diversity

MDPI

Article

Cladocera (Crustacea: Branchiopoda) of Man-Made Lakes at the Northeast Part of the United Arab Emirates with a Hypothesis on Their Origin

Alexey A. Kotov [1,*], Anna N. Neretina [1], Shamma Eisa Salem Al Neyadi [2], Dmitry P. Karabanov [3] and Waleed Hamza [2,*]

[1] A.N. Severtsov Institute of Ecology and Evolution, 119071 Moscow, Russia
[2] Department of Biology, College of Science United Arab Emirates University (UAEU), Al Ain Abu Dhabi 15551, United Arab Emirates
[3] I.D. Papanin Institute for Biology of Inland Waters, 152742 Borok, Russia
* Correspondence: alexey-a-kotov@yandex.ru (A.A.K.); w.hamza@uaeu.ac.ae (W.H.)

Abstract: A study of the water fleas (Crustacea: Cladocera) in man-made lakes in the northeast part of the United Arab Emirates revealed five species: *Ceriodaphnia* cf. *cornuta* Sars, 1885; *Daphnia (Ctenodaphnia) arabica* Neretina, Al Neyadi et Hamza, 2022; *Moina* cf. *micrura* Kurz, 1875; *Anthalona mediterranea* (Yalim, 2005); *Coronatella anemae* Van Damme et Dumont, 2008. The morphologies of the four taxa are described in detail, except that of *D. Arabica*, which has been described previously. The phylogenies of the *C. cornuta* and *M. micrura* species groups were reconstructed based on sequences of the COI mitochondrial gene and the possible divergence age of the Arabian clades was estimated based on molecular clocks with paleontological calibration. We concluded that the *C. cornuta* complex was differentiated in the Upper Jurassic to Lower Cretaceous. The splitting off of clades containing the Arabian population took place during the Oligocene to Miocene. The *M. micrura* species group was differentiated in the Upper Cretaceous, and the splitting off of clades including Arabian populations took place around the Oligocene. Therefore, the clades (of different hierarchical orders) in the Arabian Peninsula are very old compared to clades of similar rank in northern Eurasia, which usually have Late Pleistocene history. Most of our sampled water bodies were newly constructed man-made reservoirs. As revealed, the phylogroups are locally distributed, and we hypothesized that they are colonists from surrounding natural water bodies inhabited by the relicts of older fauna that survived after the great climate aridization and then occupied newly available (man-made) biotopes.

Keywords: water fleas; phylogeny; molecular clocks; COI

Citation: Kotov, A.A.; Neretina, A.N.; Al Neyadi, S.E.S.; Karabanov, D.P.; Hamza, W. Cladocera (Crustacea: Branchiopoda) of Man-Made Lakes at the Northeast Part of the United Arab Emirates with a Hypothesis on Their Origin. *Diversity* **2022**, *14*, 688. https://doi.org/10.3390/d14080688

Academic Editors: Maciej Karpowicz, Carlos López and Michael Wink

Received: 24 July 2022
Accepted: 19 August 2022
Published: 21 August 2022

1. Introduction

The study of the organism diversity on our planet is regarded as an important direction in the biological sciences; its importance is reflected in several international documents, including the Convention on Biological Diversity [1]. Many recent scientific publications have focused on the general patterns of the distribution of biodiversity, its global and local hotspots [2–4], which are important for biogeographic generalizations, and the history of biodiversity pattern formation [5,6]. However, there are still many insufficiently studied regions, especially in areas with extremely arid climates [7]. The Arabian Peninsula is an example of a region with such a climate, exhibiting a relatively small number of shallow continental water bodies and relatively scarce fauna and flora [8,9].

Several groups of microscopic animals are present in almost all continental water bodies, and water fleas (Crustacea: Cladocera) are among such groups [10]. The cladocerans are a model group for various fields of the biological sciences: biogeography, ecology, molecular biology, etc. [11–16]. Only a few studies on the cladocerans of the Arabian Peninsula have been published to date, mainly from Yemen [17,18]. Arid territories in

northern Africa have been investigated by well-known European carcinologists since the second half of the 19th century [19–25]. As a result, we have adequate information on the cladoceran species composition there. In recent years, such studies are often conducted by local hydrobiologists in cooperation with European colleagues [26–28]. Socotra Island is adequately studied mainly due to the efforts of Kay Van Damme [29,30].

The United Arab Emirates is a country bordered by the Gulf of Oman and the Arabian Gulf, while its southern neighbours are Saudi Arabia and Oman. "UAE's particular environment—hot and dry—greatly limits the country's biodiversity richness" [1]. Most of the country belongs to Ecoregion 443, "Oman Mountains" [31,32], but such subdivision seems to be too coarse with respect to the UAE because the same area belongs to four different terrestrial ecoregions [33]. A few studies on the animals inhabiting the desert water bodies have been conducted to date, including studies on fish [34], snails [35], ostracods [36] and fairy shrimps [37]. Recently, research on the fauna of continental waters has been intensified in this country [8,36,38]; some alien freshwater species were found [39], and many of the native UAE species are threatened by invasive alien species [8].

However, only two publications on the cladocerans are known to date [40,41], and some specimens were also analysed after hatching from mud collected in the UAE [29,42]. Recently, we described an endemic taxon of *Daphnia* (*Ctenodaphnia*) Dybowski et Grochowski from this region and demonstrated that the region played an important role in the differentiation of the cladoceran taxa and their subsequent colonization of more northern territories [43]. Here, we provide details on the Cladocera collected in several dams from the north-eastern portion of the United Arab Emirates. The aim of our study was to carry out a morphological analysis of all the cladocerans found and determine the biogeographic status of two common taxa with sequences well-represented in Genbank [44] and BOLD [45] based on their molecular phylogenies.

2. Materials and Methods

2.1. Sampling and Morphological Analysis

The sampling sites are marked by arrows in Figure 1a. Photos of the sampled water bodies are shown in Figure 1b–d. The samples were collected qualitatively in winter in six localities with five water bodies (Figure 1 and Table 1, localities 1–3, 5–6). Standard plankton nets were used to collect the samples from the littoral and pelagic zones of each water body, and ca. 1000 litres were filtered each time. Material collected in the field was fixed in 4% formaldehyde or 96% ethanol immediately after sampling. No accompanying physico-chemical analyses were made as the ecological problems were out of our scope. Some specimens were hatched from resting eggs from dried mud collected in the dried locality 4 (see description of culture starting from resting eggs in previous publications [40,43]). Whole samples were kept in the collection of the Department of Biology, College of Science, United Arab Emirates University, UAE. Selected specimens were kept in the collection of the A.N. Severtsov Institute of Ecology and Evolution, Russia.

For morphological analysis, the whole samples were examined, and then selected specimens of the water fleas were picked from the samples and tentatively identified under an MBS-10 binocular stereoscopic microscope (LOMO-Microsystems, St. Petersburg, Russia) based on taxonomic keys [42,46,48]. Detailed investigation of specimens was carried out under an Olympus BX41 optical microscope (Olympus Corporation, Tokyo, Japan) with higher magnification. When necessary, specimens were dissected using tungsten needles and diagnostic body parts were investigated in separate drops of glycerol. The line drawings were prepared using a *camera lucida* attached to the Olympus BX 41. Some specimens were dehydrated and dried according to a standard protocol [49], coated with gold in a Q150R ES Plus (Quorum Technologies Ltd., East Sussex, UK) and investigated under a Tescan Mira 3 LMH scanning electron microscope (Tescan, Brno, Czech Republic). For morphological description, we used the terminology summarized and discussed by Kotov [49].

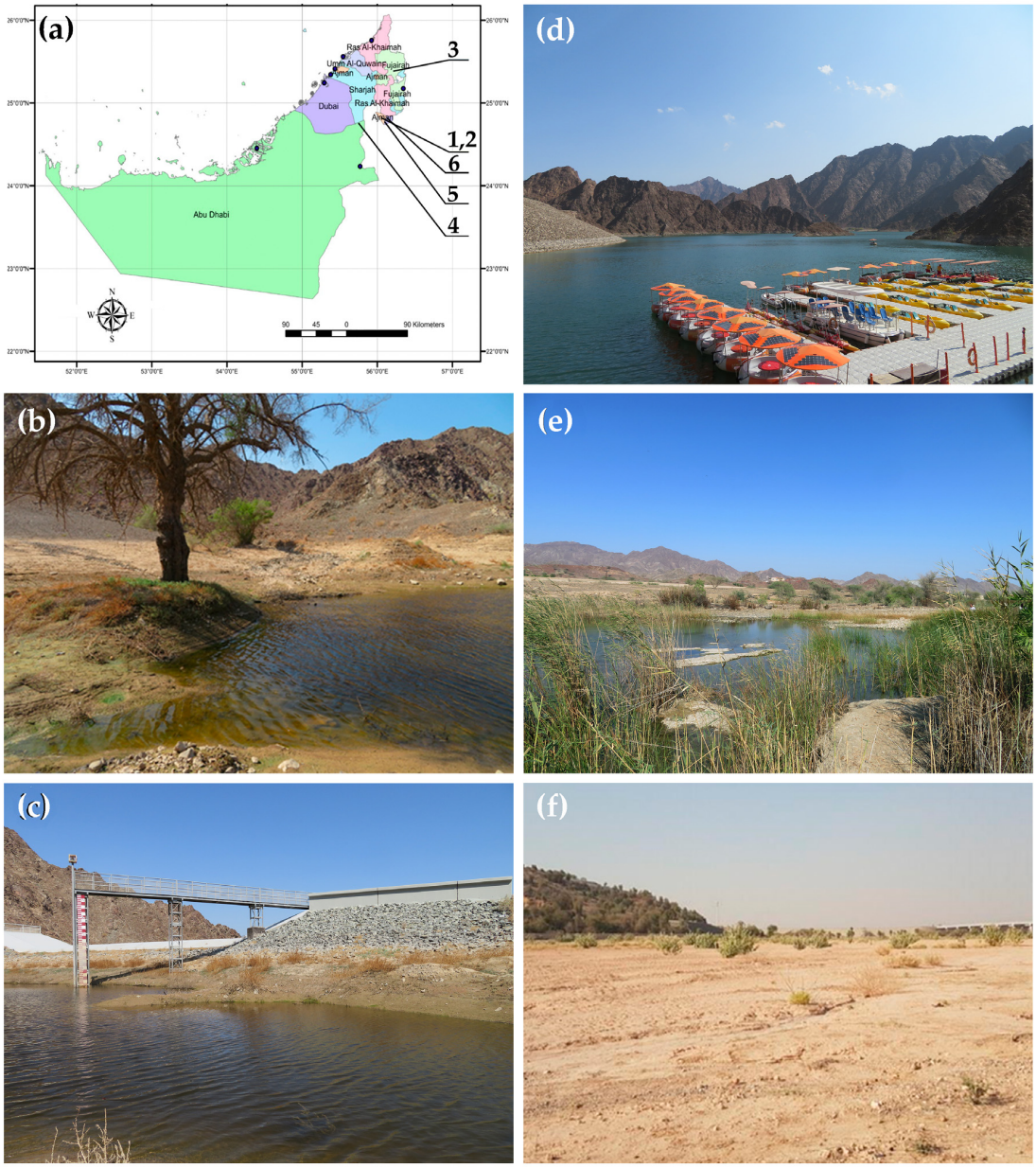

Figure 1. Map of UAE with sampled sites (**a**) and photos of the sites on 28 October 2019: (**b**) locality 1: Kholaiban Dam Masfut 1; (**c**) locality 2: Kholaiban Dam Masfut 2; (**d**) locality 5: Hatta Dam; (**e**) locality 6: Sheikh Maktoum Bin Rashid Al Maktoum Dam; (**f**) locality 4: Al Shuwaib Dam, dried at time of sediment collection.

Table 1. List of localities where the different taxa were collected.

№	Emirate	Locality	N	E	*C. c.*	*D. a.*	*M. m.*	*A. m.*	*C. a.*
1	Ajman	Kholaiban Dam Masfut 1	24.81019	56.09278	1	0	1	1	1
2	Ajman	Kholaiban Dam Masfut 2	24.80982	56.09306	0	0	1	0	0
3	Fujairah	Wadi Maidaq—Blue Pool	25.35205	56.08864	0	0	1	1	1
4	Abu Dhabi	Al Shuwaib Dam, near Al Ain city	24.77174	55.80146	0	1	0	0	0
5	Dubai	Hatta Dam	24.7835	56.11186	0	0	0	0	0
6	Dubai	Sheikh Maktoum Bin Rashid Al Maktoum Dam	24.81213	56.1469	0	0	0	0	0

Table abbreviations: ***C.c.***—*Ceriodaphnia* cf. *cornuta*; ***D.a.***—*Daphnia arabica*; ***M.m.***—*Moina* cf. *micrura*; ***A.m.***—*Anthalona mediterranea*; ***C.a.***—*Coronatella anemae*.

2.2. Abbreviations

In illustrations and text: I–V = thoracic limbs I–V; e1–e5 = endites 1–5 of the thoracic limbs; ejh = ejector hooks on limb I; epp = epipodite; ext = exopodite; IDL = inner distal lobe of limb I; ODL = outer distal lobe of limb I; pep = preepipodite; s = sensillum.

In phylogenetic reconstructions: ML—maximum likelihood; MP—maximum parsimony; BI—Bayesian interference.

2.3. Genetics

DNA extraction was performed from two specimens of *C.* cf. *cornuta* and two specimens of *Moina* cf. *micrura* initially identified by their morphological characters. Genomic DNA was extracted from single adult parthenogenetic females using the Wizard Genomic DNA Purification Kit (Promega Corp., Madison, WI) according to the manufacturer's protocol. As a genetic marker, we used the 5′-fragment of the first subunit of mitochondrial cytochrome oxidase (COI), this being a standard locus for DNA-based animal identification [50].

Amplification was performed using previously published protocols [47,51]. Initial analysis of the chromatograms, formation of contigs and their subsequent editing were undertaken with the Sanger Reads Editor in UniprouGENE v.42 [52]. All original sequences were verified by BLAST comparisons with published cladoceran sequences in the NCBI BLAST nr/nt database [53]. The sequences from this study were submitted to the NCBI GenBank database (accession numbers ON437588 and ON496457). Sequences of specimens from other regions were taken from GenBank (Supplementary Table S1). The alignment was carried out using the MAFFT v.7 algorithm [54] realized in the uGENE package. Substitution models were selected using ModelFinder v.1.6 [55] from the webserver of the Center for Integrative Bioinformatics Vienna (CIBIV), Austria [56]; the substitution model was identified for each (first, second and third) nucleotide position in the codon, and substitution models were selected based on minimal values of the Bayesian information criterion (BIC) [57]. All selected models demonstrated convergence according to the BIC and AICc, providing additional evidence for the model fit. The models of nucleotide substitutions were similar and identified as follows: for *Ceriodaphnia*, 1st COI—TNe + I, 2nd COI—F81 + F, 3rd COI—HKY + F + G4; for *Moina*, 1st COI—TNe + I + G4, 2nd COI—F81 + F + I, 3rd COI—TIM2 + F + G4.

Phylogenetic reconstruction was carried out using the three (maximum likelihood, parsimony and Bayesian) most popular methods [58], based on "unlinked" data for each locus and nucleotide position in each codon, and then a consensus tree for all "unlinked" datasets was built. Joining of all sequences into a single dataset and formation of the nexus files were performed in SequenceMatrix v.1.7. [59].

ML analysis was conducted using IQ-TREE v.2.2 [60]. To estimate the branch support values, we used 1000 replicas of the bootstrap test with ultra-fast bootstrapping in UFboot2, which requires less resources and demonstrates higher effectiveness as compared to traditional support tests [61]. To conduct a topology test, we used the SH-aLRT fast algorithm [62] in the CIBIV server.

MP reconstruction was undertaken using the "new" ultrafast algorithm TNT v.1.5 [63], with New Technology sectorial search (with RSS and CSS) and tree fusing settings. To perform the branch support test, we used 1000 replicas of a standard bootstrap test.

For BI analysis, we used the multi-taxon coalescence model "star" [64] in the software package BEAST2 v.2.6 [65] with all of the parameters of the substitution model determined using BEAUti [66]. In each analysis, we conducted six independent runs of a Markov chain Monte Carlo (MCMC) simulation (20,000,000 generations, with selection of each 10,000th generation).

As a prior outgroup, we used sequences of *Daphnia* published by Cornetti et al. [67]. The effectiveness of the MCMC runs, taking into consideration the estimations of the effective size (ESS) for all parameters higher than 200, was controlled in Tracer v.1.7 [68]. After unification of MCMC runs using LogCombiner (part of BEAST2), a consensus tree was obtained in TreeAnnotator (part of BEAST2) with a burn-in rate 25%. Posterior probabilities

were used as support values, following the recommendations from [69]. As the main clades for all trees were congruent, we presented the ultrametric BI trees, with branch support for key nodes.

For estimation of the possible divergence age of different clades, we used molecular clocks with paleontological calibration [70] instead of the complicated methods based on mathematic modelling. We used calibration points [67] with 15% standard deviation: *Daphnia/Ctenodaphnia* (approx. 175.4 MYA), *D. longispina*/*D. pulex* (133.9 MYA), *D. similis*/*D. sinensis* (64.1 MYA), *D. magna* (Europe)/*D. magna* (Asia) (9.3 MYA). Age of lineage divergence was estimated based on the optimized relaxed clock model in the "ORC" package for BEAST2 [71]. This algorithm has several optimizations to improve the statistical accurateness of the "relaxed" molecular clocks, as well as increasing the productivity of such calculations. The Yule model of speciation was selected as maximally adequate for the data on several species [72]. Further analysis was conducted according to the recommendations of Barido-Sottani et al. [73].

Species delimitation was undertaken based on three approaches. The first, based on genetic distances, utilized the ASAP application on the webserver of the Atelier de BioInformatique, France [74]. The delimitation pattern was identified based on the best value of the "asap-score", with minimal "P-val".

The second approach was based on a general mixed Yule-coalescent model (GMYC) [75]. We used the Bayesian GMYC model in the "bGMYC" package [76] for "Microsoft R-Open and MKL", 64-bit v.3.5.3 [77]. For the bGMYC analysis, we randomly selected 100 ultrametric trees from the 1000 trees after burn-in from BEAST2 (see above). To avoid a prejudicial estimation, the thinning interval was determined as 100, and number of possible tips was identical to the general number of sequences. The number of MCMC generations used was 100,000, with a burn-in of 50%, and the range of threshold values was from 2 to the maximum number of sequences in the dataset; start values for both Yale and coalescence models were set to those which, according to Reid and Carstens [76], are the most usable for the majority of datasets. The results were accepted as statistically significant at a modified $p > 0.95$, a level which should significantly reduce the likelihood of excessive "fragmentation" in the designation of taxonomic structure [78].

The third method of species delimitation was based on Poisson tree processes (PTPs). For data processing, we used multi-rate Poisson tree processes (mPTPs) [79] on the webserver of the Heidelberg Institute for Theoretical Studies (HITS), Germany. As the input tree for mPTP analysis, we used both the BI tree from BEAST2 and the ML tree obtained using IQ-TREE. The topologies of the two trees and their conclusions on species delimitation were identical in both cases; the presence or absence of the outgroup did not change the conclusions.

3. Results

3.1. Morphological Account

3.1.1. *Ceriodaphnia cf. cornuta*

Family Daphniidae Straus, 1820

Genus *Ceriodaphnia* Dana, 1853

***Ceriodaphnia* cf. *cornuta* Sars, 1885**

Figures 2–4.

Material examined. Two parthenogenetic females from locality 1, coll. 28 December 2019 by S.E.S. Al Neyadi; four parthenogenetic females from locality 1, coll. 21 January 2020 by S.E.S. Al Neyadi; en parthenogenetic females from locality 1, coll. 11 February 2021 by S.E.S. Al Neyadi.

Parthenogenetic female. In lateral view, body rounded, typical of the genus; body height/length = 0.68, maximum height in middle (Figures 2a and 3a,b). Dorsum of valves broadly convex, with prominent dorsolateral depression between head and the rest of body. Posterodorsal angle projected, but without a caudal needle. Ventral margin broadly rounded, smoothly passing to anteroventral margin. No integumental hairs on head and

valves (Figure 3a–f). Body moderately compressed laterally, subovoid in dorsal or ventral view. Any lateral protuberances absent.

Head (Figures 2b–d and 3c–e) small, with a prominent beak-like "rostrum"(which is probably not homologous to the rostrum of *Daphnia*, see [49]) and a voluminous ocular dome surrounding a large compound eye (Figures 2b–d and 3d–g). Minute ocellus rounded or slightly elongated, located near base of antenna I. Frontal head pore not found (Figure 3h,i). Dorsal head pore absent (Figure 2a,b). Labrum (Figure 2e) with a wide, fleshy main body and a large, setulated distal labral plate.

Valve (Figures 2f–i and 4a) large, almost rounded, with a prominent polygonal ornamentation on the outer surface (Figures 2i, 3a–f and 4b). From inner side, ventral margin with a series of relatively long setae, covered by fine setulae (Figure 2h). Posteriorly, this row fluently turns to a series of setulae (Figures 2g,h and 4a).

Thorax relatively long, abdomen short.

Postabdomen (Figures 2j–k and 4c–e) elongated, subovoid. Ventral margin almost straight or slightly concave. Large anus located subdistally. Preanal margin long and slightly convex or straight (Figure 2j–k). Anal margin three times shorter than preanal margin. Preanal and anal margins bear seven to nine pairs of sharp teeth twice longer than the diameter of the base of the postabdominal claw and provided with a group of small setulae at their base. Laterally, series of small denticles are located above the row of spines on the anal portion. Small additional bunches of setulae on dorsal and lateral sides of preanal portion. Postabdominal seta (Figure 2a,j) as long as postabdomen, its distal and proximal segments subequal in length; distal segment covered by short, fine setulae. Postabdominal claw (Figures 2k and 4e–g) massive, evenly curved, with particularly sharp, pointed tip. On outer side of claw, two successive pectens along the dorsal margin, proximal one consisting of thin, small denticles and distal one also consisting of thin, small denticles decreasing in length distally, the proximal ones being larger than those of the proximal pecten.

Antenna I cylindrical, swollen and short (length about three diameters), without prominent rows of setulae (Figures 2l and 3g–i). Antennular sensory seta slender, twice longer than the antenna I body, arising subdistally from an inflated protuberance. Nine short subequal aesthetascs in size (Figure 2l).

Antenna II long (Figures 2b, 3b,c,f and 4h). Coxal part with two short sensory setae; basal segment robust, covered by transverse rows of hairs, with a distal sensory seta on anterior face (Figure 2b). Antennal branches elongated with all segments cylindrical, covered by rows of short hairs; first endopod segment almost as long as the three first exopod segments. Antennal formula: setae 0-0-1-3/1-1-3; spines 0-0-0-0/0-0-0. On both exopod and endopod branches, there are three long, apical swimming setae, all with basal and distal segments bilaterally feathered by fine, long setulae (Figure 2b). Lateral setae of exopod and endopod have the same armature. Apical spines absent.

Thoracic limbs typical of the genus (see Alonso et al. [80]), see limb I in Figure 4i.

Size. Adult parthenogenetic females up to 0.70 mm in length.

Variability. No significant variability was found in studied individuals.

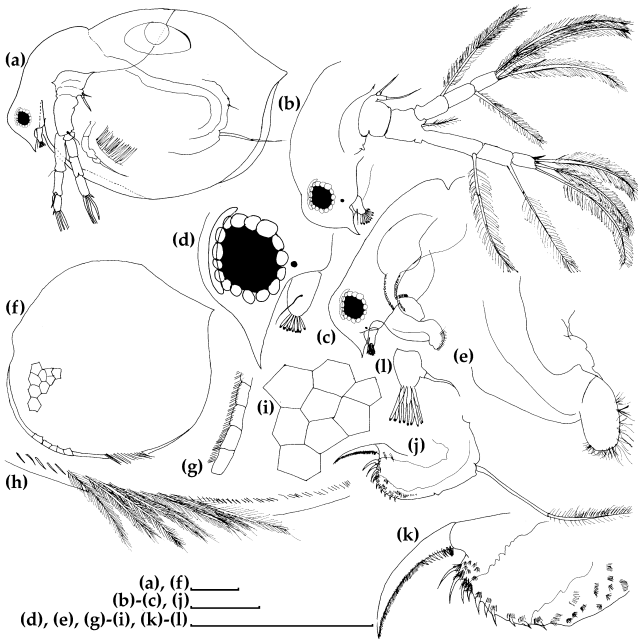

Figure 2. *Ceriodaphnia* cf. *cornuta*, an adult parthenogenetic female from Masfoot Dam 1, United Arab Emirates. (**a**) Female, lateral view; (**b**–**d**) head, lateral view; (**e**) labrum; (**f**) valve, lateral view; (**g**) armature of posterior margin of valve, inner view; (**h**) armature of ventral margin of valve, inner view; (**i**) ornamentation of lateral portion of valve, outer view; (**j**) postabdomen; (**k**) postabdominal claw; (**l**) antenna I; All scale bars: 0.1 mm.

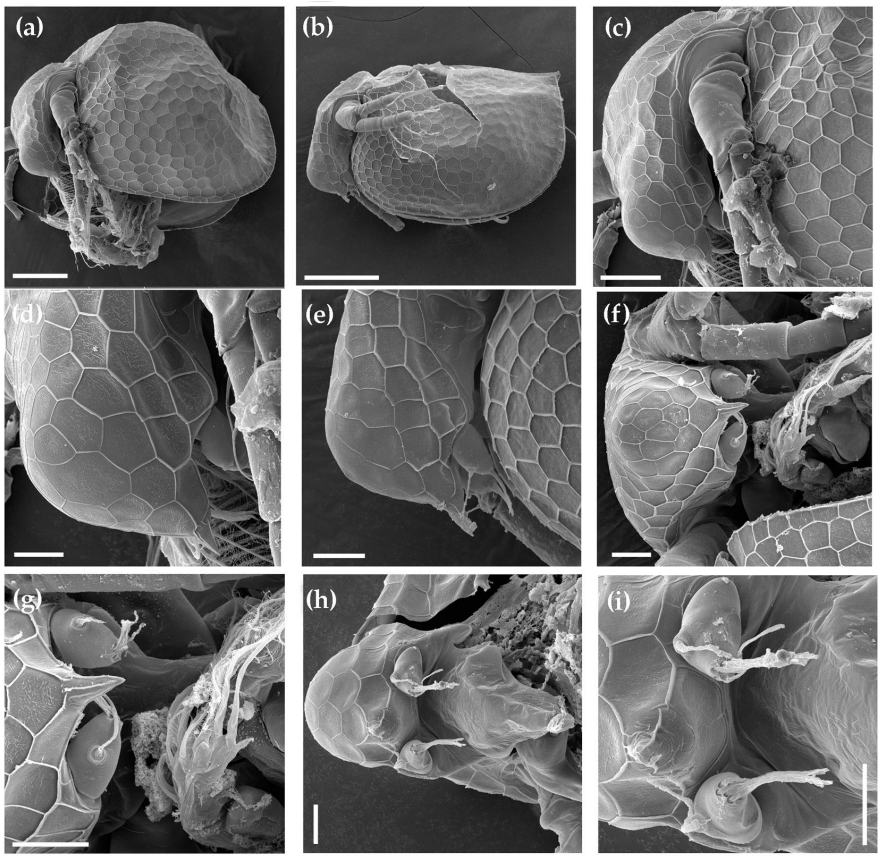

Figure 3. *Ceriodaphnia* cf. *cornuta*, adult parthenogenetic females from Masfoot Dam 1, United Arab Emirates. (**a**,**b**) adult females, lateral view; (**c**–**e**) head, lateral view; (**f**) head, ventral view; (**g**) rostrum, ventral view; (**h**,**i**) antenna I. Scale bars: 0.1 mm for (**a**,**b**), 0.05 mm for (**c**), 0.02 mm for (**d**–**i**).

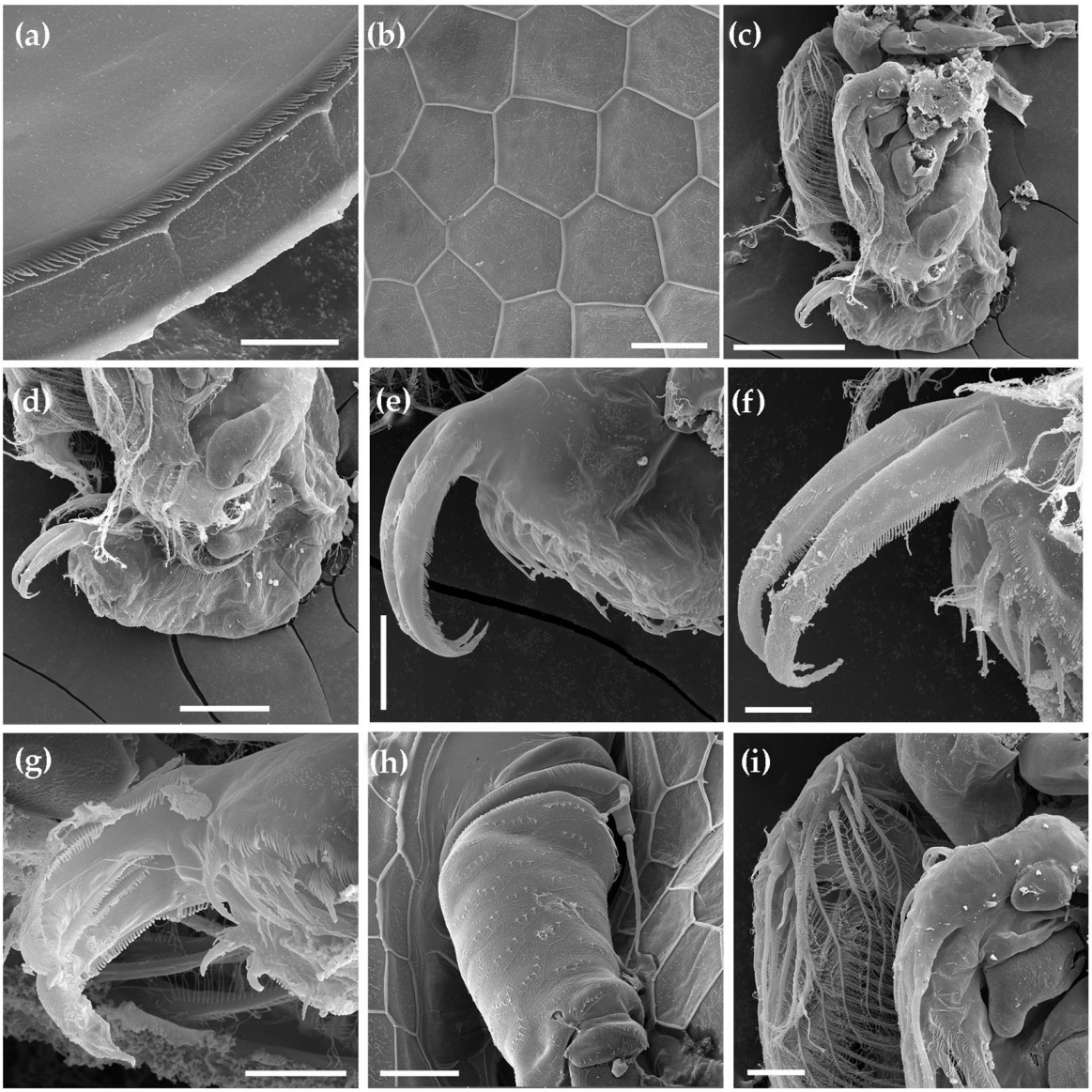

Figure 4. *Ceriodaphnia* cf. *cornuta*, an adult parthenogenetic female from Masfoot Dam 1, United Arab Emirates. (**a**) Armature of posterior margin of valve, inner view; (**b**) ornamentation of lateral portion of valve, outer view; (**c**) thoracic limbs and postabdomen, cut off from the rest of the body; (**d**) postabdomen; (**e**,**f**) postabdominal claws, lateral view; (**g**) postabdominal claws, dorsal view; (**h**) basal portion of antenna II; (**i**) limb I; Scale bars: 0.1 mm for (**c**), 0.05 mm for (**d**), 0.02 mm for (**b**), (**h**,**i**), 0.01 for (**a**,**e**–**g**).

3.1.2. *Daphnia (Ctenodaphnia) arabica*

Family Daphniidae Straus, 1820
Genus *Daphnia* O.F. Müller, 1776
Subgenus *Ctenodaphnia* Dybowski et Grochowski, 1895
***Daphnia (Ctenodaphnia) arabica* Neretina, Al Neyadi et Hamza, 2022**
Figures 5 and 6.

Material examined. Many parthenogenetic females, ephippial females and males of the laboratory culture hatched from the mud from locality 4.

Description. See Hamza et al. [43].

Comments. See Hamza et al. [43].

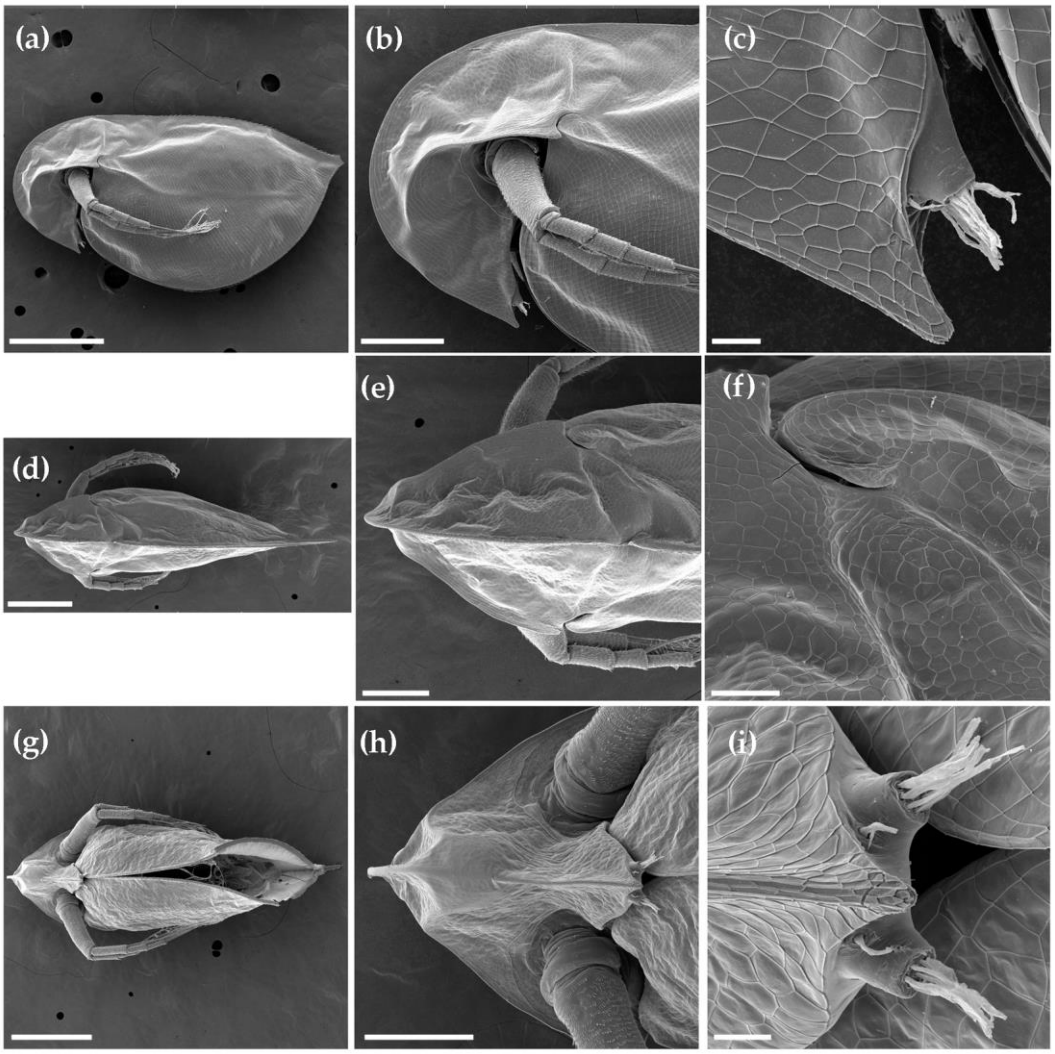

Figure 5. *Daphnia arabica*, adult parthenogenetic females from Al Shuwaib Dam, near Al Ain city, United Arab Emirates. (**a**) Female, lateral view; (**b**) head, lateral view; (**c**) rostrum and antenna I; (**d**) female, dorsal view; (**e**) head, dorsal view; (**f**) head, dorsal view on higher magnification; (**g**) female, dorsal view; (**h**) head, ventral view; (**i**) head, ventral view on higher magnification. Scale bars: 0.5 mm for (**a**,**d**,**g**), 0.2 mm for (**b**,**e**,**h**), 0.05 mm for (**f**), 0.02 mm for (**g**,**i**).

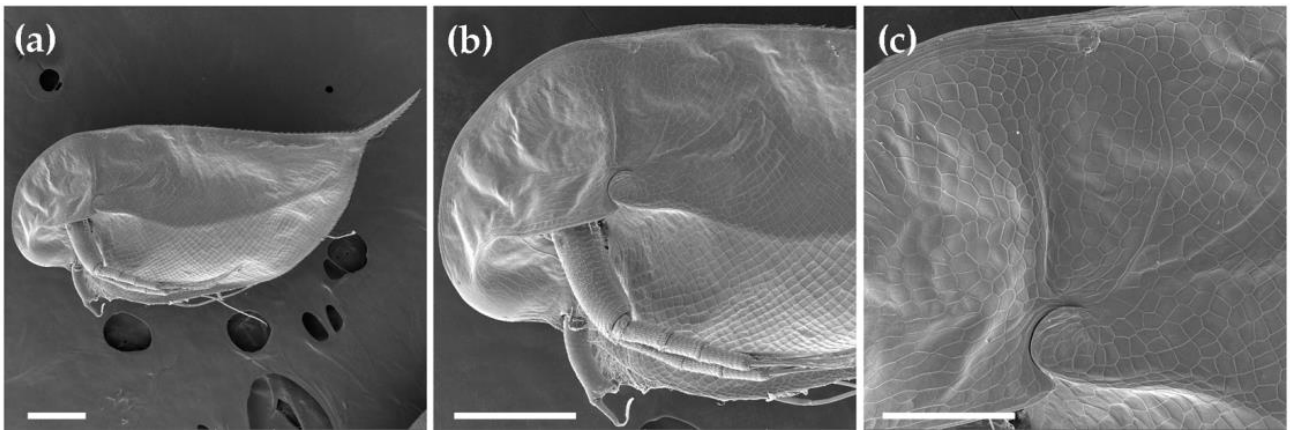

Figure 6. *Daphnia arabica*, an adult male from Al Shuwaib Dam, near Al Ain city, United Arab Emirates. (**a**) Male, lateral view; (**b**) head; (**c**) head with higher magnification. Scale bars: 0.2 mm for (**a**,**b**), 0.1 mm for (**c**).

3.1.3. *Moina* cf. *micrura*

Family Moinidae Goulden, 1968
Genus *Moina* Baird, 1850
***Moina* cf. *micrura* Kurz, 1875**
Figures 7–10.

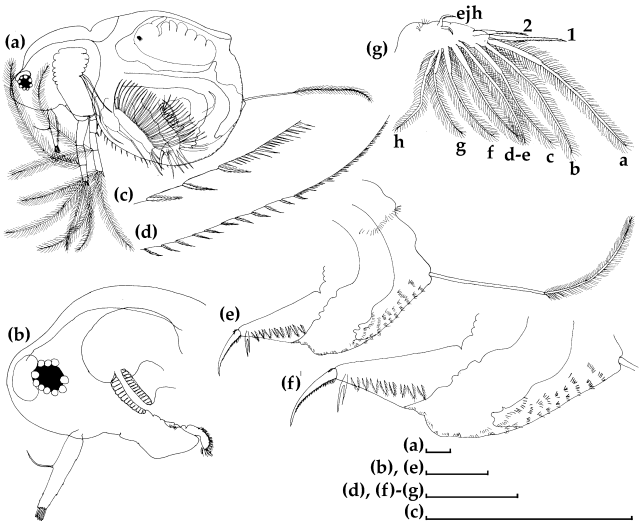

Figure 7. *Moina* cf. *micrura*, an adult parthenogenetic female from Masfoot Dam 1, United Arab Emirates. (**a**) Female, lateral view; (**b**) head; (**c**,**d**), armature of posteroventral portion of valve, inner view; (**e**,**f**), postabdomen; (**g**) thoracic limb I. All scale bars: 0.1 mm.

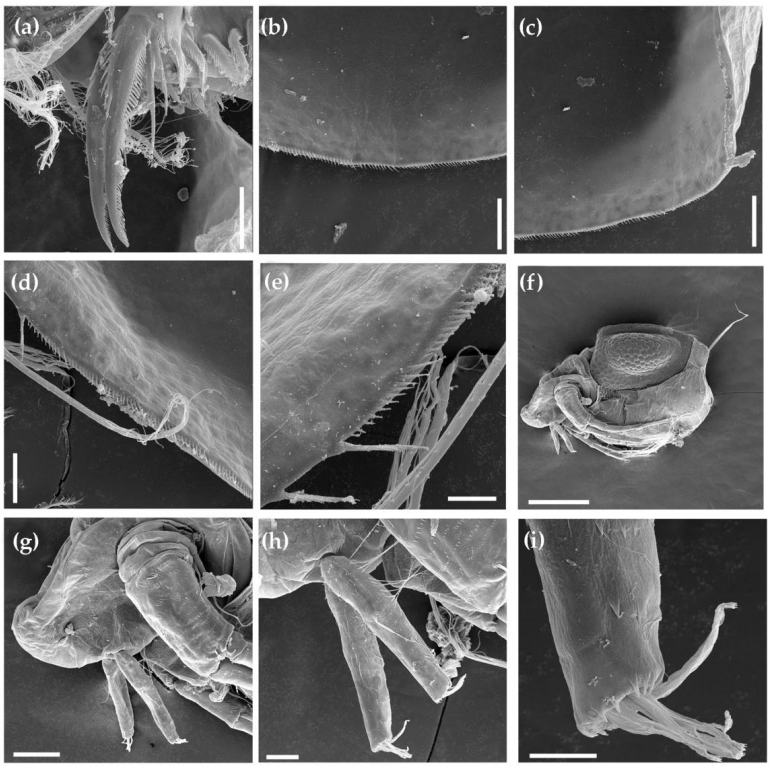

Figure 8. *Moina* cf. *micrura*, parthenogenetic (**a**–**e**) and ephippial (**f**–**i**) females from Masfoot Dam 1, United Arab Emirates. (**a**) Postabdominal claws, ventral view; (**b**,**c**), armature of posterior margin of valve, inner view; (**d**,**e**), armature of posteroventral margin of valve, inner view; (**f**) ephippial female, lateral view; (**g**) head; (**h**) antenna I; (**i**) antenna I with higher magnification. Scale bars: 0.2 mm for (**f**), 0.05 mm for (**g**), 0.02 mm for (**a**–**d**,**h**), 0.01 mm for (**e**,**i**).

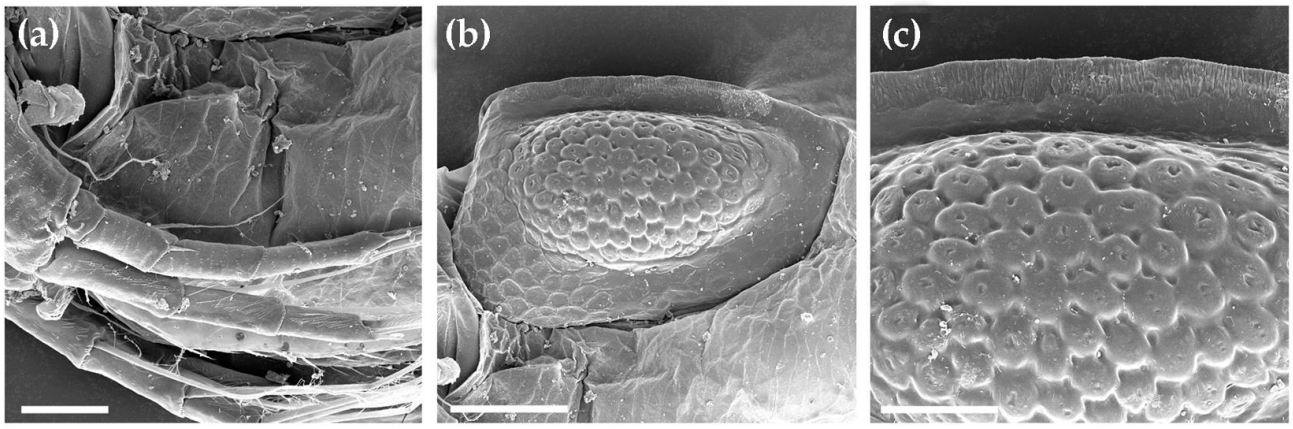

Figure 9. *Moina* cf. *micrura*, an ephippial female from Masfoot Dam 1, United Arab Emirates: (**a**) antenna II; (**b**) ephippium; (**c**) ornamentation of ephippium with higher magnification. Scale bars 0.1 mm for (**b**), 0.05 mm for (**a**,**c**).

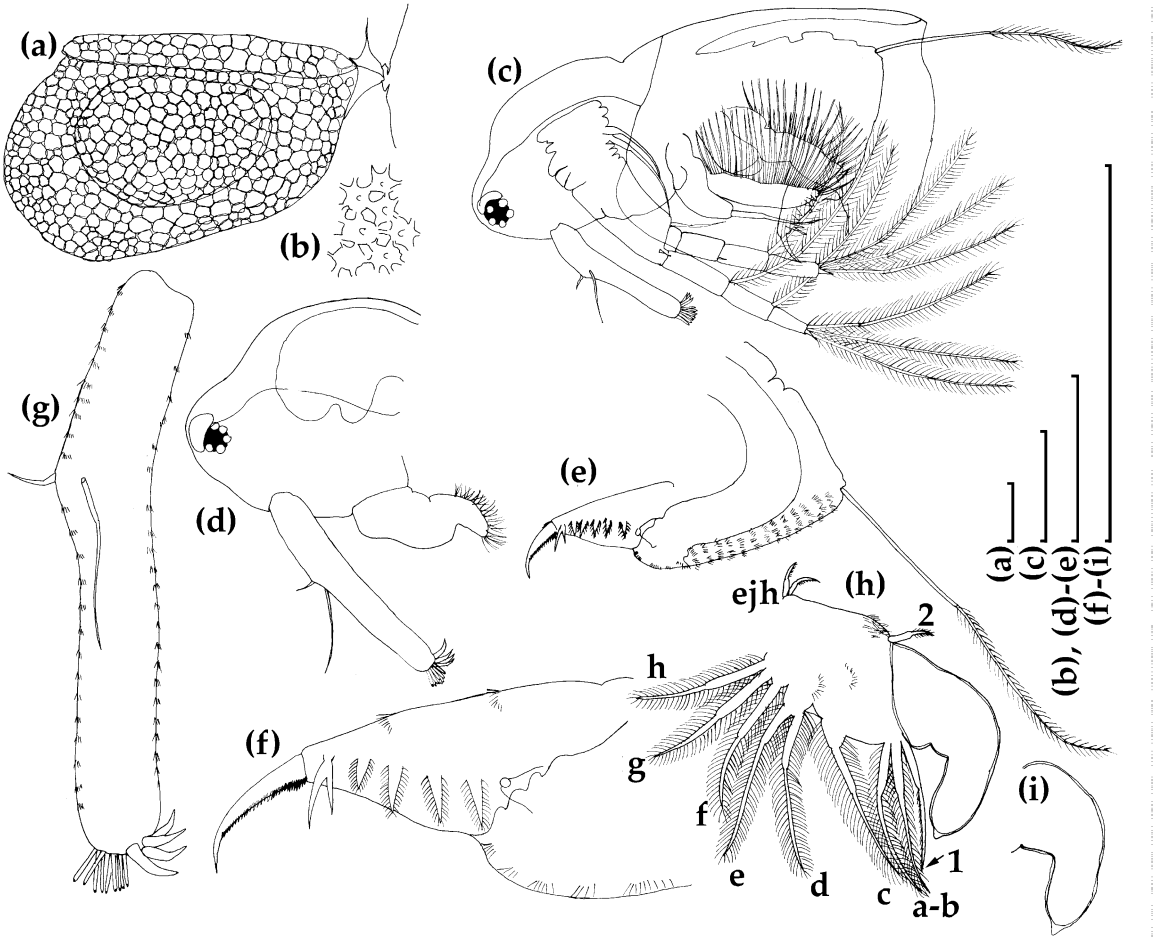

Figure 10. *Moina* cf. *micrura*, an ephippium (**a**,**b**) and an adult male (**c**–**i**) from Masfoot Dam 1, United Arab Emirates. (**a**) Ephippium, lateral view; (**b**) ornamentation of ephippium with higher magnification; (**c**) male, lateral view; (**d**) head; (**e**,**f**) postabdomen; (**g**) antenna I; (**h**) thoracic limb I; (**i**) copulatory hook. All scale bars: 0.1 mm.

Material examined. Two parthenogenetic females from locality 1, coll. 28 October 2019 by S.E.S. Al Neyadi; four parthenogenetic females from locality 1, coll. 21 January 2020 by S.E.S. Al Neyadi; three parthenogenetic females, four ephippial females from locality 2,

coll. 28 October 2019 by A.A. Kotov, A.N. Neretina and W. Hamza; six parthenogenetic females, two ephippial females from locality 2, coll. 28 October 2019 by A.A. Kotov, A.N. Neretina and W. Hamza; three parthenogenetic females, three ephippial females from locality 2, coll. 28 October 2019 by A.A. Kotov, A.N. Neretina and W. Hamza; two parthenogenetic females from locality 3, coll. 28 October 2019 by S.E.S. Al Neyadi.

Parthenogenetic female. Body ovoid in lateral view, moderately low for genus (body height/length = about 0.62), maximum height in middle portion (Figure 7a). Dorsum of valve somewhat elevated behind head. Shallow dorsolateral depression separates head from rest of body. Posterodorsal angle prominent, rounded, posteroventral angle broadly rounded. Ventral margin moderately convex. Anterodorsal angle prominent, rounded. Very fine sculpture on valves, forming cells elongated in dorsoventral direction, no integumental hairs on head and valves. Body moderately compressed laterally in anterior view.

Head relatively large, with prominent supra-ocular depression and massive compound eye (Figure 7b). Ocellus absent. Head pores absent. Labrum with fleshy main body, its ventral margin slightly concave, labral plate densely setulated (Figure 7b). Valve large, broadly ovoid (Figure 7a). Anterior portion of ventral margin provided with moderately long setae covered by tiny setulae (Figure 7c), posterior margin with a row of setulae, grouped in its ventral portion (Figures 7d and 8b–e).

Thorax relatively long. Abdomen short.

Postabdomen elongated, conically narrowing distally (Figure 7e,f); ventral margin almost straight, with rows of minute setulae. Preanal margin long, convex, gradually passing to anal margin. Preanal and anal portions covered by rows of minute setulae (Figure 7f). Postanal portion conical, both distal margin and dorsodistal angles not expressed. Laterally postanal portion of postabdomen bearing a row of 8–10 large, triangular, plumose teeth. Anteriormost tooth bidentate, with branches unequal in length. Postabdominal setae slightly longer than postabdomen (Figure 7a). Postabdominal claw large, slightly curved, with pointed tip (Figures 7e and 8a), its outer lateral side with a group of somewhat larger denticles at base of claw.

Antenna I thin (length approximately equal to six diameters of antennular body base), long, slightly curved (Figure 7b); surface covered by numerous fine, long setae and rows of minute denticles (Figure 8g,h). Antennular sensory seta slender, arising almost at middle of antennular body; nine short aesthetascs almost subequal in size (Figure 9i).

Antenna II large and long; coxal part with three setulated sensory setae subequal in length (Figure 7a). Basal segment robust, with short distal spine on outer surface between antennal branches and long seta on inner surface; this segment covered by numerous transverse rows of fine denticles and long setae. Antennal branches elongated. Exopod 4-segmented, subequal in size to 3-segmented endopod. All branch segments cylindrical, with rows of small denticles and setae. Antennal formula: setae 0-0-1-3/1-1-3, spines 0-1-0-1/0-0-1. Lateral and apical swimming setae of both antennal branches covered by long, fine setulae. Spine on second exopod segment short, comparable in length to both apical exopod and endopod spines.

Thoracic limbs as in other members of the *Moina micrura* species complex [81].

Limb I (Figure 7g) with elongated, narrow corm; inner distal lobe (or endite 5 sensu Kotov [49]) with a single anterior seta (Figure 7g: 1), bearing short setulae, and two soft setae (Figure 7g: a,b). Armature of posterior soft setae similar in all limbs: both segments provided with fine, long setulae. Endite 4 with single, relatively short anterior seta, and single posterior seta (Figure 7g: 2, c). Endites 3 with 2 posterior setae, without anterior setae (Figure 7g: d,e). Endites 2 with 3 posterior setae (Figure 7g: f–h). Two ejector hooks of remarkably different sizes. No maxillar process (or endite 1 sensu Kotov [49]) on limb base.

Ephippial female. Body shape and appendages of ephippial female (Figures 8f–i and 9a–c) appearing similar to those of parthenogenetic female, but with dorsal portion transformed into ephippium (Figures 8f and 9b,c), casting off during the moulting and surrounding a single resting egg (Figure 10a). Dorsal part of valves with reinforced dorsal chitinous plate expanded to centre in dorsal view. Ephippium yellow-brownish. Macrosculpture of ephippium as polygonal

swollen cells at the centre (Figure 10b) and polygonal flat cells along the rim, these features well-recognizable both under light and scanning electron microscopy. Microsculpture as tiny dots visible only under scanning electron microscope (Figure 9b,c); some wrinkles on dorsal plate (Figure 9c).

Male. In lateral view, body ovoid, more elongated compared to female (body height/length about 0.57) (Figure 9c). Dorsal margin of valves slightly elevated above head, posteroventral angle distinct.

Head longer than in female; labrum somewhat smaller than that of females, with a large, setulated distal labral plate (Figure 9d). Head pores absent. Compound eye large. Ocellus absent. Valve ovoid, more elongated than that in female, with short setae, decreasing in size posteriorly, along ventral margin.

Thorax, in contrast to parthenogenetic and gamogenetic, relatively long. Abdomen short.

Postabdomen generally as in female, with large bidentate tooth distally (distal branch always significantly larger than basal branch), and row of seven to nine large, triangular plumose teeth (Figure 10e,f). Gonopore opening in lateral surface of postabdomen. Postabdominal setae almost two times longer than postabdomen. Its distal segment significantly longer than proximal one.

Antenna I very long and regularly curved, covered by tiny hairs and rows of small denticles (Figure 10g). Antennular sensory seta long, arising from first quarter of antennular body. Male seta more robust, located near sensory seta. Apical tip of antennular body separated into two parts: first with 9 short aesthetascs, second with four pointed hooks.

Thoracic limb I essentially similar to that in parthenogenetic female but bearing a large, curved copulatory hook with setulated margin and pointed apex (Figure 10h,i).

Size. Adult parthenogenetic females up to 0.95 mm in length; ephippial females up to 0.93 mm in length; adult males up to 0.45 mm in length.

Variability. No significant variability was found in individuals between localities.

3.1.4. *Anthalona mediterranea*

Family Chydoridae Dybowski et Grochowski, 1894 emend. Frey, 1967
Subfamily Alanine Dybowski et Grochowski, 1894 emend. Frey, 1967
Genus *Anthalona* Van Damme, Sinev et Dumont, 2011
***Anthalona mediterranea* (Yalim, 2005)**
Figures 11–15.

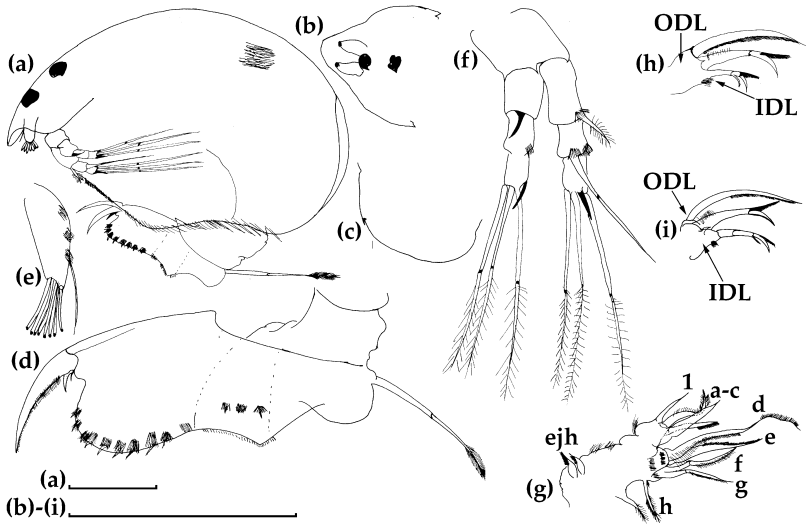

Figure 11. *Anthalona mediterranea*, an adult parthenogenetic female from Wadi Maidaq—Blue Pool, United Arab Emirates. (**a**) Female, lateral view; (**b**) anterior portion of head, dorsal view; (**c**) labral keel; (**d**) postabdomen; (**e**) antenna I; (**f**) antenna II; (**g**–**i**) thoracic limb I (schematically). All scale bars: 0.1 mm.

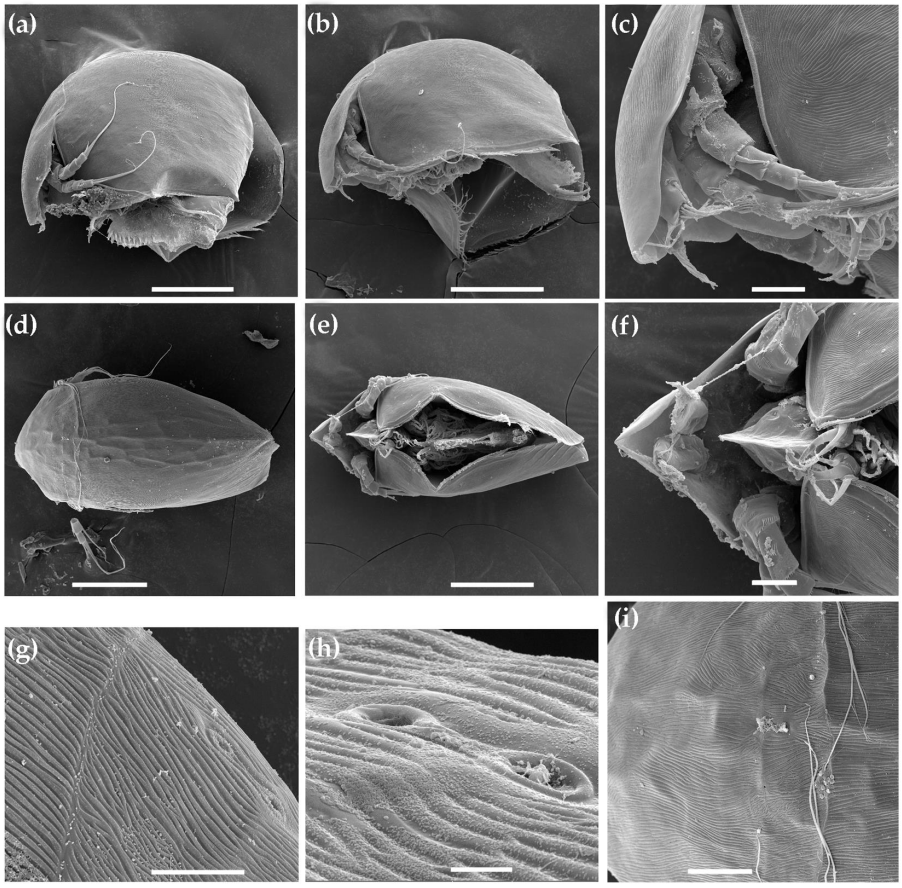

Figure 12. *Anthalona mediterranea*, adult parthenogenetic females from Wadi Maidaq—Blue Pool, United Arab Emirates. (**a**,**b**), Female, lateral view; (**c**) head, lateral view; (**d**) female, dorsal view; (**e**) female, ventral view; (**f**) head, ventral view; (**g**), ornamentation of dorsal part of head; (**h**) main head pores; (**i**) lateral and main head pores. Scale bars: 0.1 mm for (**a**,**b**,**d**,**e**), 0.02 mm for (**c**,**f**,**i**), 0.01 mm for (**g**), 0.002 mm for (**h**).

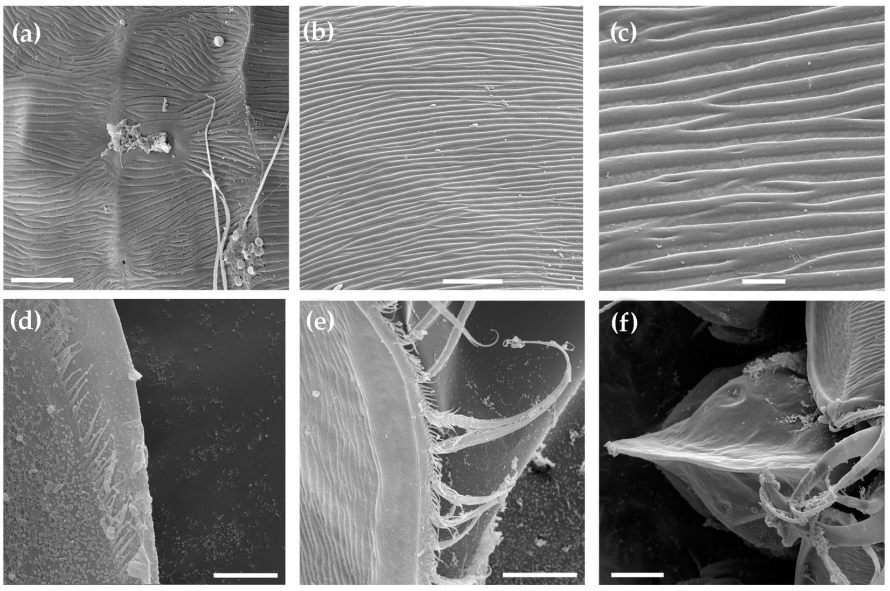

Figure 13. *Anthalona mediterranea*, an adult parthenogenetic female from Wadi Maidaq—Blue Pool, United Arab Emirates. (**a**) Lateral and main head pores; (**b**,**c**) ornamentation of valves, outer view; (**d**) ornamentation of valve, posterior portion, inner view; (**e**) ornamentation of valve, ventral portion, inner view; (**f**) labral keel, ventral view. Scale bars: 0.01 mm for (**a**,**b**,**e**,**f**), 0.005 mm for (**d**), 0.002 mm for (**c**).

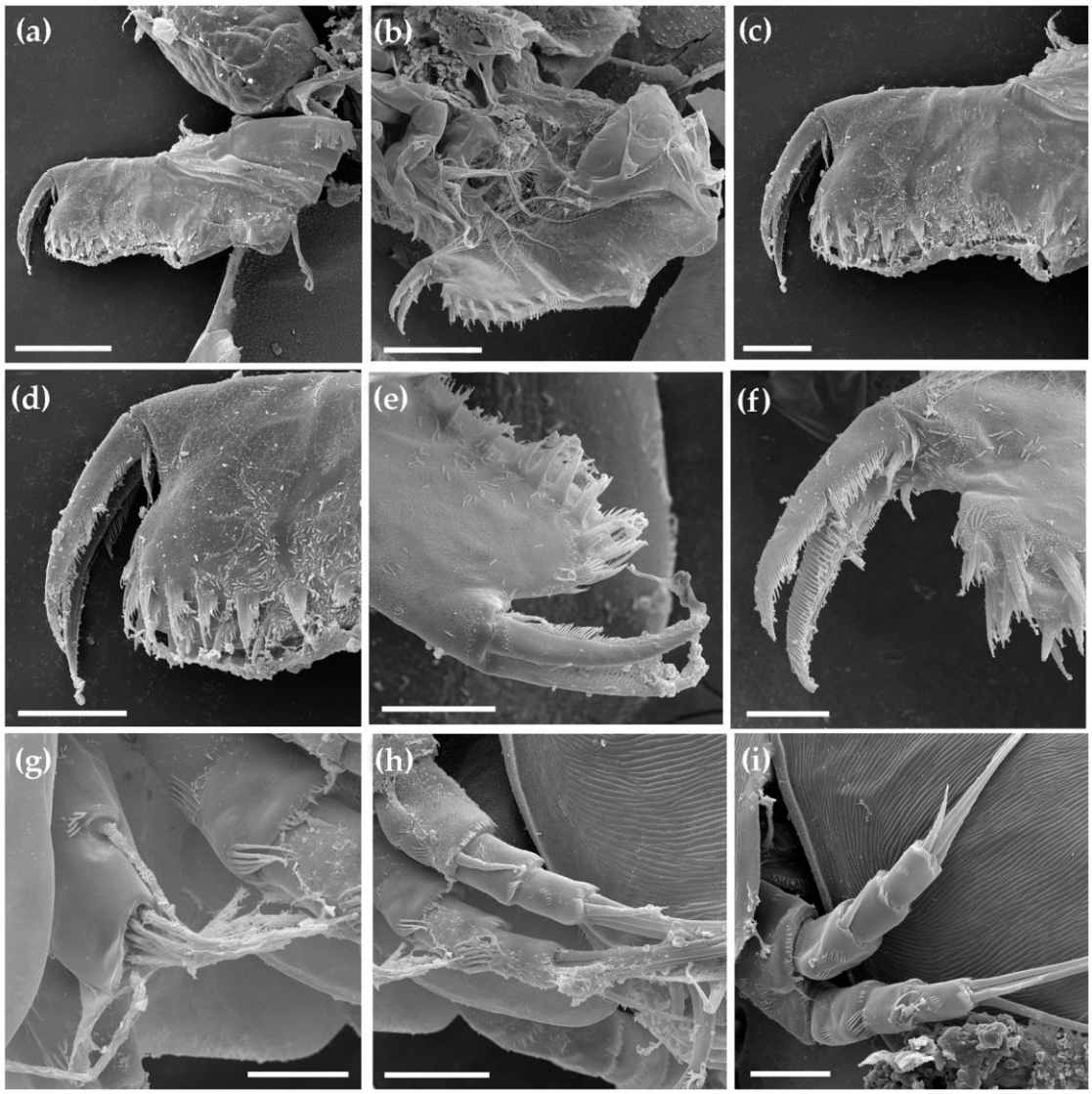

Figure 14. *Anthalona mediterranea*, an adult parthenogenetic female from Wadi Maidaq—Blue Pool, United Arab Emirates. (**a**–**c**) Postabdomen, lateral view; (**d**–**f**) postabdominal claws; (**g**) antenna I; (**h**,**i**) antenna II. Scale bars: 0.05 mm for (**a**,**b**), 0.02 mm for (**c**–**e**,**h**,**i**), 0.01 mm for (**f**,**g**).

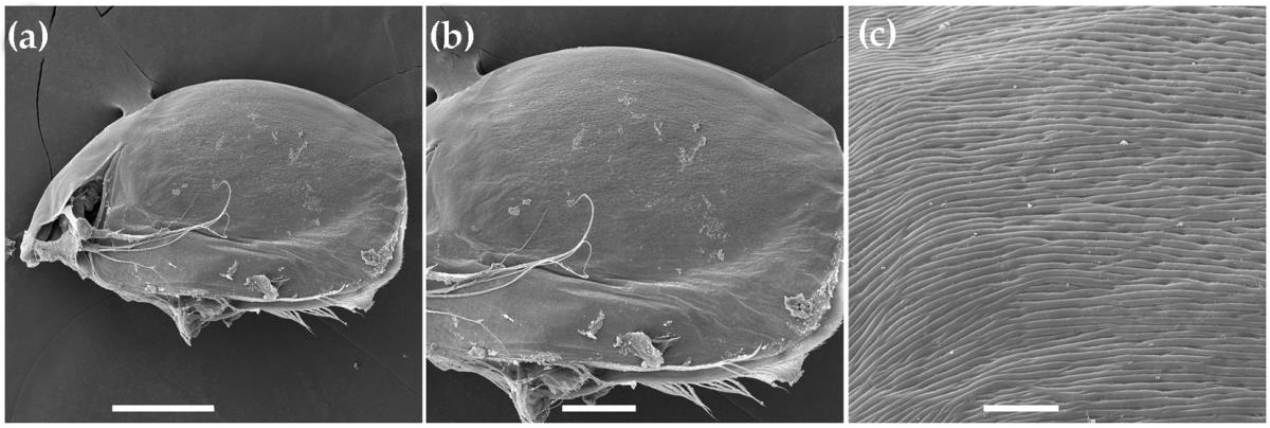

Figure 15. *Anthalona mediterranea*, an ephippial female from Wadi Maidaq—Blue Pool, United Arab Emirates: (**a**) female, lateral view; (**b**) ephippium; (**c**) ephippium with higher magnification. Scale bars: 0.1 mm for (**a**), 0.05 mm for (**b**), 0.01 mm for (**c**).

Material examined. Five parthenogenetic females from locality 1, coll. 21 January 2020 by S.E.S. Al Neyadi; five parthenogenetic females from locality 1, coll. 11 February 2021 by S.E.S. Al Neyadi; ten parthenogenetic females, five ephippial females, two males from locality 3, coll. 1 April 2019 by S.E.S. Al Neyadi; two parthenogenetic females and two ephippial females from locality 3, coll. 21 January 2020 by S.E.S. Al Neyadi.

Adult parthenogenetic female. In lateral view, body ovoid, sometimes slightly yellowish. Dorsum moderately convex, with highest point in middle; posterior margin moderately convex (Figures 11a and 12a,b). Ventral margin moderately convex. Posteroventral corner round, without notches or denticles. Body moderately compressed laterally (Figure 12d,e).

Head small. Ocellus subequal in size to compound eye (Figure 11a). Rostrum well-developed, broadly rounded (Figures 11b and 12c,f). Head shield with two main head pores, interpore distance long (Figure 12g–i). Two lateral pores represented by cosmaria; sacks under small pores large, their circular size about twice that of a main head pore (not illustrated here, see Van Damme et al., 2011). Labrum with a single denticle at labral keel (Figure 11c), with small paired depressions on body (Figure 13f).

Valve with ornamentation as a striation (Figures 12g–i and 13a–c). A series of setulae in middle of ventral margin (Figure 13e), only minute setulae at posterior margin (Figure 13d).

Postabdomen not widening distally, widest at level of preanal angle, and with a rounded dorsodistal margin. Length 2–2.5 times width (Figures 11d and 14a–d). Ventral margin straight. Preanal, anal and postanal margins of subequal length. Anal margin concave, postanal margin distinctly convex. Distal margin not protruding, distal embayment dorsally to claw basis maximally as deep as claw width at base (Figure 14d–f). Preanal angle triangular, not protruding far beyond maximal dorsal point of margin (neither postanal margin nor preanal corner reach dorsally beyond each other). Postanal teeth in groups of six to seven. Each distal tooth with adjacent smaller elements on anterior side, partly merged towards distal end of postabdomen. Lateral setae in six fascicles in postanal portion, consisting of four to six elements in each group, parallel to each other. Most distal lateral elements in postanal portion reach half their size beyond the marginal teeth. Smaller elements per fascicle at least half as long as distal most spiniform element in each group (Figure 14d–f). Three to four clusters of smaller marginal teeth, close to each other, almost a continuously armed anal margin, and three to four fascicles in anal portion. Postabdominal claw (Figure 14a–f) longer than anal margin of postabdomen, moderately curved, covered by setulae along dorsal side. Proximal pecten ending in long spine about width of claw at this point and just under half of claw length. Basal spine short, just about claw width at base and about one sixth of claw length. Group of three to four thick, short basal spinules, about half of basal spine length.

Antenna I (Figures 11e and 14g) about 2.5 times long as wide, sensory seta arising from one third of antenna I body. Three to four series of short setulae on margin. Longest aesthetascs slightly longer than half of antenna I corm, shortest half as long.

Antenna II (Figures 11f, 12c and 14h,i) with a spine on basal segment, relatively large, conical. A series of short spinules at base of first exopod segment. First exopod seta on antenna II narrow, not reaching distal margin of distal exopod segment, second exopod seta twice as long as previous; on external side of second exopod segment, two groups of three strong spiniform setulae (Figure 14h,i). Spine on first endopod segment not longer than second segment; main terminal spines on endo- and exopod branches well-developed, each as long as its apical segment or just shorter. Terminal setae on antennal exopod strongly modified: they are chitinized and thickened. Shortest seta most spiniform, about as long as three exopod segments together. Exopod strongly bent. Apical setae on endopod slender and with long setulae.

Thoracic limbs as described by Van Damme et al. [42]. Thoracic limb I (Figure 11g–i) identical to type population. Accessory seta present. Outer distal lobe (Figure 11h,i: ODL) with a single slender seta, as long as largest seta of inner distal lobe (Figure 11h,i: IDL) and with strong setulae in distal half; two setae of inner distal lobe with modified and chitinized distal halves. Largest seta of inner distal lobe with a single large spine followed by spines

decreasing in size distally and reduced distal part (Figure 11h,i: IDL); spine in longest seta of inner distal lobe mostly longer than distal part beyond it. On the shortest seta of inner distal lobe, two long spines of similar size, basal spine as long as distal part.

Ephippial female. It is larger than parthenogenetic female, ephippium dark brown, with a sole resting egg and somewhat thinner sculpture (Figure 15a–c) as compared to parthenogenetic female.

Male. In lateral view, body rectangular-rounded (Figure 16a). Head in general as in female (Figure 16b,c). Postabdomen (Figure 16d,e) about two times as long as wide, with a strongly developed triangular preanal projection. Distalmost spine in each lateral fascicle on postabdomen long and reaching beyond dorsal margin of postabdomen. Terminal claw thick and short (shorter than anal margin) with basal spine about one fourth of terminal claw length. Gonopores opening ventrally, adjacent to the basis of postabdominal claw.

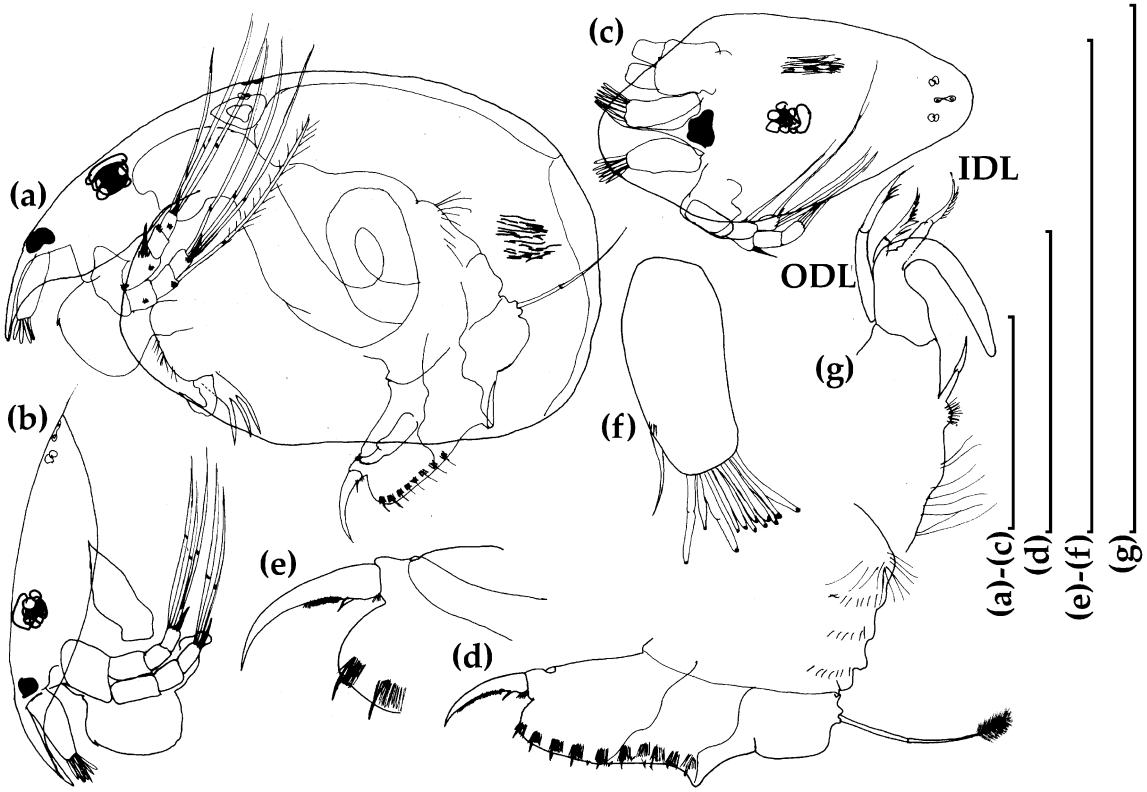

Figure 16. *Anthalona mediterranea*, an adult male from Wadi Maidaq—Blue Pool, United Arab Emirates. (**a**) Male, lateral view; (**b**) head, lateral view; (**c**) head, dorsal view; (**d**) postabdomen, lateral view; (**e**) postabdominal claw, lateral view; (**f**) antenna I; (**g**) thoracic limb I, fragment. All scale bars: 0.1 mm.

Antenna I shorter than in female, with a sensory seta as in female; terminally with 12 aesthetascs and an additional male seta shorter than shortest aesthetasc (Figure 16f).

Thoracic limb I with inner distal lobe bearing three setae, of which two modified in distal portion, though less than in female (Figure 16g). Third seta of inner distal lobe naked, longer than each of two modified setae. Copulatory hook strongly curved and short, in inner side with broad base and U-shaped, distal part as long as proximal part.

Size. Adult parthenogenetic females up to 0.55 mm in length; ephippial females up to 0.58 mm in length; adult males up to 0.35 mm in length.

Variability. No significant variability was found in individuals between localities.

3.1.5. *Coronatella anemae*

Family Chydoridae Dybowski et Grochowski, 1894 emend. Frey, 1967
Subfamily Aloninae Dybowski et Grochowski, 1894 emend. Frey, 1967
Genus *Coronatella* Dybowski et Grochowski, 1894

Coronatella anemae **Van Damme et Dumont, 2008**
Figures 17–20.

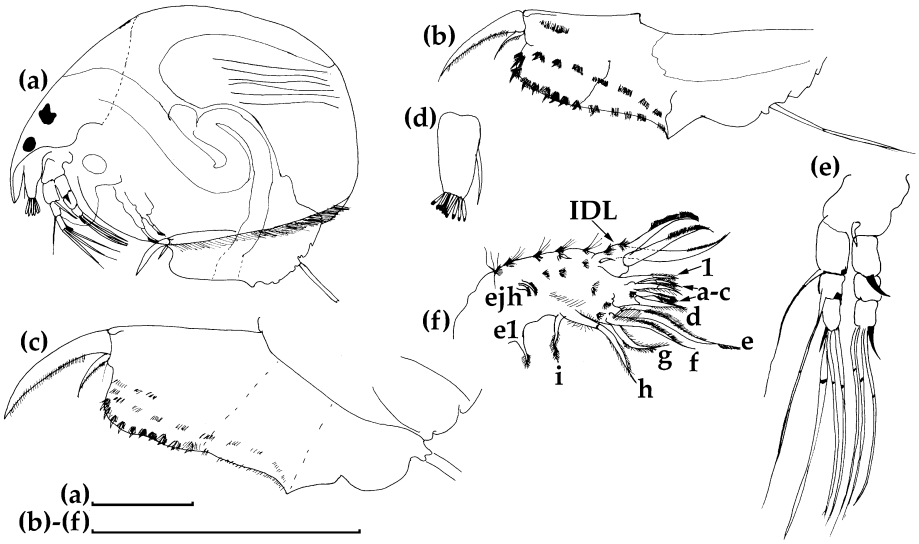

Figure 17. *Coronatella anemae*, an adult parthenogenetic female from Wadi Maidaq—Blue Pool, United Arab Emirates. (**a**) Female, lateral view; (**b**,**c**) postabdomen; (**d**) antenna I; (**e**) antenna II; (**f**) thoracic limb I. All scale bars: 0.1 mm.

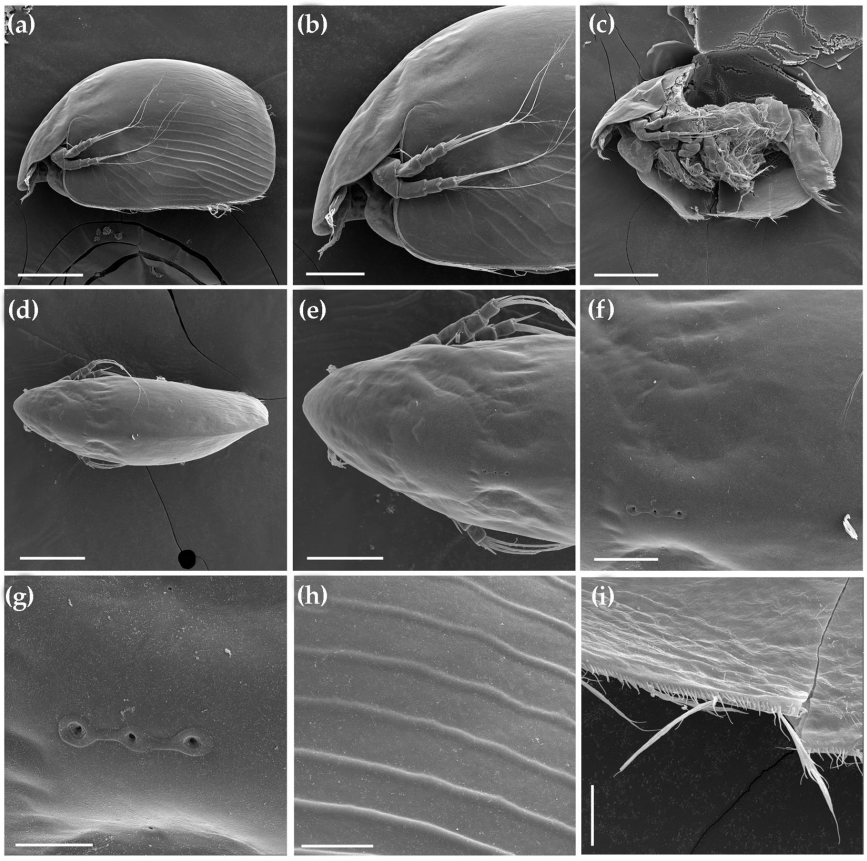

Figure 18. *Coronatella anemae*, an adult parthenogenetic female from Wadi Maidaq—Blue Pool, United Arab Emirates. (**a**) Female, lateral view; (**b**) head, lateral view; (**c**) dissected female, lateral view; (**d**) female, dorsal view; (**e**) head, dorsal view; (**f**,**g**) head pores; (**h**) ornamentation of posterior portion of valve, outer view; (**i**) armature of ventral margin of valve, inner view. Scale bars: 0.1 mm for (**a**,**c**,**d**), 0.05 mm for (**b**,**e**), 0.02 mm for (**f**,**h**), 0.01 mm for (**g**,**i**).

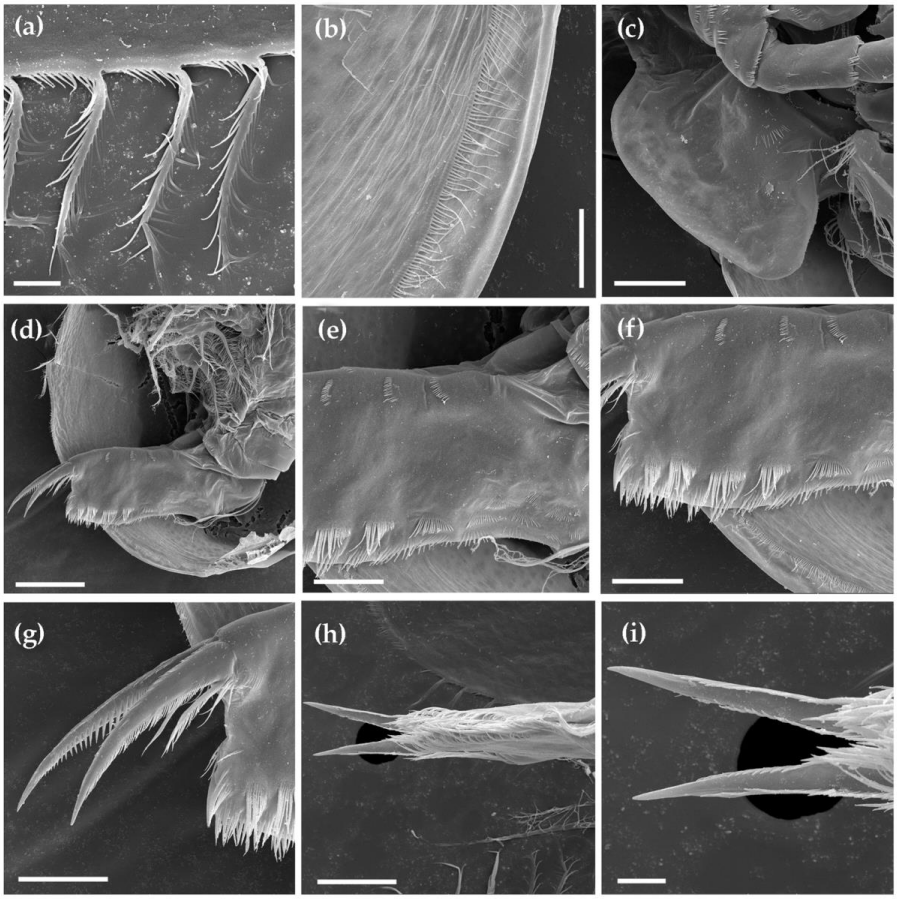

Figure 19. *Coronatella anemae*, an adult parthenogenetic female from Wadi Maidaq—Blue Pool, United Arab Emirates. (**a**) Armature of ventral margin of valve, inner view; (**b**) armature of posterior margin of valve, inner view; (**c**) labrum; (**d**) postabdomen; (**e**,**f**) armature of postabdomen with higher magnification; (**g**) postabdominal claws, lateral view; (**h**,**i**) postabdominal claws, dorsal view. Scale bars: 0.05 mm for (**d**), 0.02 mm for (**c**,**e**–**h**), 0.01 mm for (**b**), 0.005 mm for (**a**,**i**).

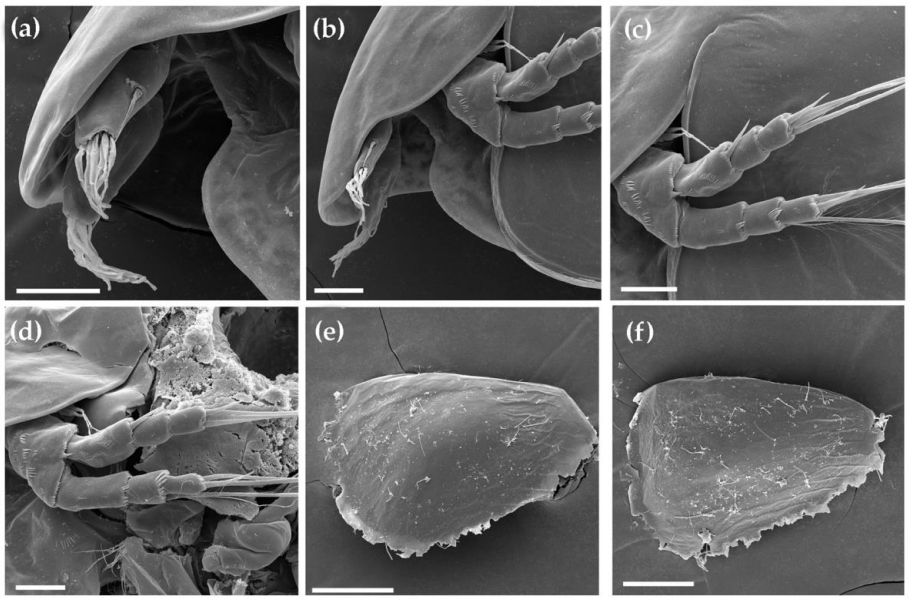

Figure 20. *Coronatella anemae*, an adult parthenogenetic female and ephippia from Wadi Maidaq—Blue Pool, United Arab Emirates. (**a**,**b**) Antenna I; (**c**,**d**) antenna II; (**e**,**f**) ephippium, lateral view. Scale bars: 0.1 mm for (**e**,**f**), 0.02 mm for (**a**–**d**).

Material examined. Two parthenogenetic females from locality 1, coll. 28 October 2019 by S.E.S. Al Neyadi; two parthenogenetic females from locality 1, coll. 21 January 2020 by S.E.S. Al Neyadi; two parthenogenetic females from locality 1, coll. 21 January 2020 by S.E.S. Al Neyadi; five parthenogenetic females from the laboratory culture hatched from locality 1; two parthenogenetic females, 1 ephippial female, 1 male from locality 3, coll. 1 April 2019 by S.E.S. Al Neyadi; 15 parthenogenetic females, 1 ephippial female, 1 male from the laboratory culture hatched from locality 3; three parthenogenetic females from locality 3, coll. 21 January 2020 by S.E.S. Al Neyadi; three parthenogenetic females from locality 3, coll. 11 February 2021 by S.E.S. Al Neyadi.

Parthenogenetic female. Body colourless, in lateral view ovoid (Figures 17a and 18a), with a regularly curved dorsal margin and rounded posterodorsal angle. Ventral margin rather straight in anterior half to slightly concave in posterior portion (Figure 17a), posteroventral corner with an unclear notch. In dorsal and ventral view, body relatively strongly compressed, but lacking a pronounced keel (Figure 18e).

Head small. Ocellus as almost large as eye (Figure 17a). Head shield broad, with rounded posterior margin (Figure 18e). Rostrum blunt and short, aesthetascs projecting beyond its tip (Figures 17a and 20a,b). Three major head pores of same size, narrowly connected; lateral pores minute (Figure 18f,g). Labral keel in lateral view relatively short, with moderately convex to wavy margin and obtuse tip (Figure 19c). A bunch of fine setulae on labral keel.

Valve with ornamentation consisting of parallel, well-developed, wide diagonal lines (Figure 18a,b,h). Posterior margin wavy. This ornamentation less developed on the head shield (Figure 18b,e). Marginal setae in different groups, relatively longer group on frontal margin of valve, followed by somewhat shorter group in middle and medium-sized group in posterior third of the margin (Figures 18i and 19a,b).

Postabdomen relatively long, about 2.5–3 times long as wide, in general subovoid (Figures 17b,c, 18c and 19d,e). Preanal, anal and postanal margins of similar length (postanal portion may be slightly longer than anal margin). Ventral margin as long as anal and postanal margin, ending abruptly before preanal corner. Postanal margin almost straight, tapering distally, distal margin protruding. Preanal corner strongly developed, triangular, protruding beyond anal and postanal margins. Marginal denticles well-developed, arranged in 8–10 groups. These marginal denticles may be relatively long (Figure 19e,f) or shorter (Figure 17c). Distal postanal marginal denticles consisting of two or more large spines, those closer to the anal margin in groups of three to four long spines, of which distal element largest. Lateral fascicles form five to seven groups in postanal portion, consisting of over 15 slender spinules in each group, parallel to each other, of similar thickness and slightly increasing in size distally. Two to three clusters of marginal denticles and double row of fascicles in anal portion.

Postabdominal claw as long as anal margin, relatively massive, slightly curved (Figures 17b,c and 19g–i), supplied with setulae along dorsal side. Long, slender basal spine, about two to three times as long as claw width at base and almost reaching half of claw length.

Antenna I about three times long as wide, sensory seta short (Figures 17d and 20a,b). Nine aesthetascs almost subequal in length.

Antenna II relatively short (Figures 17e and 20c,d). Coxal setae not studied. One spine on basal segment relatively large, prominent. Proximal exopod seta on antenna long and narrow, reaching beyond last antennal segments. Spine on first endopod segment as long as second endopod segment; main terminal spines on endo- and exopod branches well-developed, as long as distal segment (Figure 20c,d). Apical setae subequal in length (Figure 17a).

Thoracic limbs as described by Van Damme and Dumont [46]. Limb I with accessory seta. Outer distal lobe with a single slender seta about as long as longest seta of inner distal lobe (Figure 17f: IDL); inner distal lobe with two setae, third seta reduced; no chitin rings in setae; armature of these setae appearing as a pecten of strong denticles decreasing in size proximally, thickness of these denticles varying between specimens.

Ephippial female. Similar to parthenogenetic female. Ephippium ovoid, dark brownish, with a sole resting egg, with unclear striation (Figure 20e,f).

Male. Not found.

Size. Adult parthenogenetic females up to 0.59 mm in length; ephippial females up to 0.55 mm in length.

Variability. No significant variability was found.

3.2. Genetic Account

3.2.1. *Ceriodaphnia*

An ultrametric tree based on the mitochondrial gene COI for *Ceriodaphnia* is represented in Figure 21, including our original sequences belonging to a single haplotype. We have marked the major clades suggested by the multi-rate mPTP method by the numbers. There are 16 major clades moderately supported by different methods, and 14 major clades form a monophyletic *C. cornuta* complex (with some taxa identified as *C. rigaudi*), but support for this group in our tree is quite low. We do not describe clades other than the aforementioned species complex.

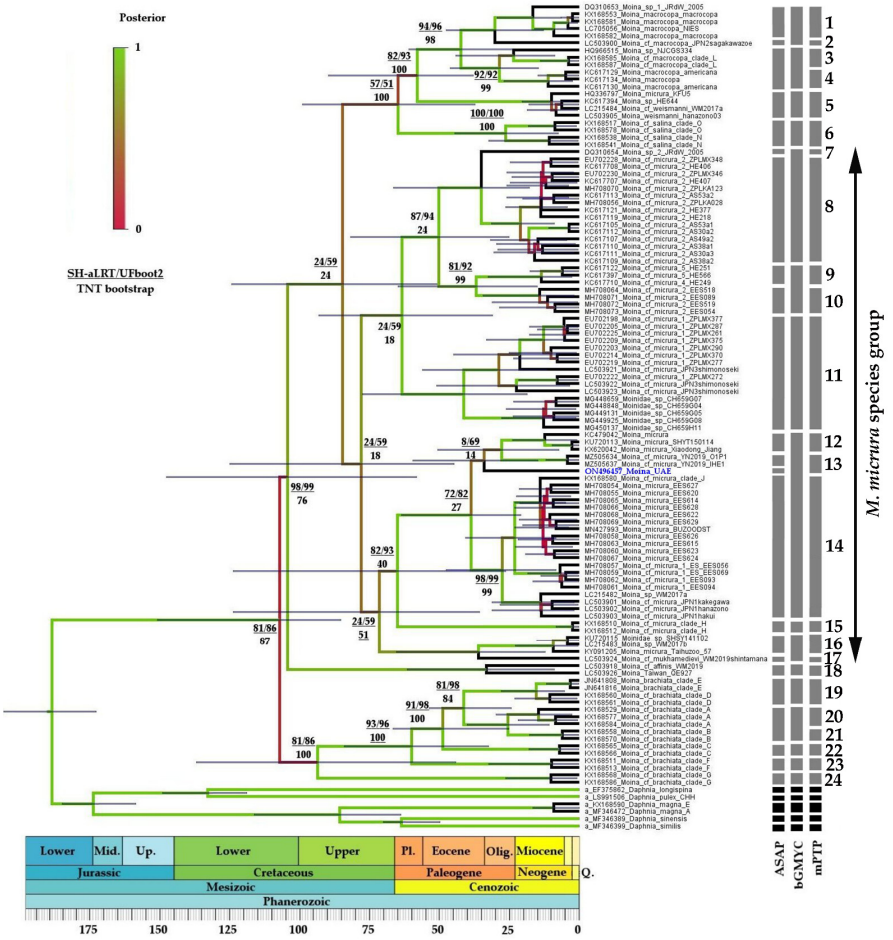

Figure 21. Phylogenetic ultrametric tree based on COI mitochondrial gene for *Ceriodaphnia* with relaxed molecular clock estimates based on fossil calibration points. Sequence from UAE is marked with blue colour. Prior probability of branches is coded by the colour gradient from red (low) to green (high). Node supports for key points are: value of the SH-aLRT for the first digit/value of UFboot2 (ML) for the second digit and standard bootstrap value in the denominator. The bars depict the 95% highest probability density (HPD) interval of the estimated divergence times. Results of delimitation based on *p*-distance (ASAP), the Bayesian general coalescence model (bGMYC) and multi-rate Poisson tree processes (mPTP) are represented by grey bars on the right side.

Clade 11 is found in Australia, China, Bangladesh, Japan and the United Arab Emirates. It groups with clade 12 from Brazil and clade 13 from Ethiopia. Finally the sister group of clades 11–13 is clade 14 from Australia, forming a fourth super-clade for the Eastern Hemisphere, but its support is low.

ASAP recognizes 13 major clades, and only clade 11 is subdivided by this analysis, into three regional groups: UAE sequences are grouped with those from China, Bangladesh and Japan vs. Australia; bGMYC gives a coarser subdivision, with nine major clades only (clades 4–6, 8–10 and 12–13 are not recognized as independent clades in this analysis).

Keeping in mind the calibration points of the *Daphnia*/*Ctenodaphnia* split at the Jurassic/Cretaceous boundary, we can roughly estimate the time of differentiation of the *C. cornuta* complex as Upper Jurassic to Lower Cretaceous; separation of the third super-clade (containing the Arabian population) took place in the Lower Cretaceous, and the splitting off of clades 11–14 took place from the Oligocene to Miocene.

Clades 1 and 2 are found in Mexico and Guatemala; together, they form a well-supported clade, grouping with clade 3 from Costa Rica with moderate support, and these three major clades (1–3) form the first large American super-clade. Clades 4–7 are also found in Mexico, forming the second American super-clade. Clade 8 from Australia is grouped with clades 9 from Thailand and 10, also from Australia, forming a third trans-continental super-clade, but support for this grouping is low.

3.2.2. *Moina*

An ultrametric tree based on the mitochondrial gene COI for *Moina* is represented in Figure 22, including our original sequences belonging to a single haplotype. Furthermore, we have marked the major clades suggested by the mPTP method by the numbers. There are 24 major clades moderately supported by different methods, and 11 major clades (7–17) form a monophyletic *M. micrura* complex, but support for this group is our tree is low. Again, we do not describe clades other than the aforementioned species complex.

Clades 1–6 represent the *M. macrocopa* group (=superclade), but its support is low. Clade 1 is found in Russia and Japan, clade 2 is found in Japan only. Mexican clade 4 is grouped with clade 3, which includes populations from the USA and Russia with high support. Highly supported clade 5 (including populations from Russia, South Korea and Japan) is grouped with clades 1–4 with relatively low support. Furthermore, highly supported clade 6 is grouped with clades 1–5 with low support.

Clades 7–17 represent the *M. micrura* group (=superclade), but it also has low support. Within this super-clade, clade 7 (represented by a population from an unknown locality) is grouped with clade 8 from Mexico. Clade 9 from Mexico is grouped with clade 10 from Spain with moderate support. Clades 7–10 are grouped with heterogeneous clade 11, including populations from Mexico, India and Japan. The next superclade joins clades 12–18. Clade 12 is found in China. Clade 13 includes populations from Nigeria and the United Arab Emirates. Clade 14 is also very heterogeneous: it includes populations from Kazakhstan, Japan, the Czech Republic, Spain and India. Clades 15–17 are more geographically compact: clade 15 includes populations from Russia, clade 16 from China and Japan and clade 17 from Japan.

Clade 18, located in Japan and Taiwan, is joined to the *M. micrura* group with high support.

The last super-clade (*M. brachiata* group) includes clades 19–24, and it has high support. Clades within this super-clade also have relatively high support and compact geographical distribution. Clade 19 includes populations from Hungary and Russia; clades 20, 22 and 23 from Russia only; and clades 21 and 24 from Russia and Mongolia.

ASAP recognizes 23 major clades, and only clade 13 from the mPTP is subdivided by this analysis, into two regional groups: UAE vs. China. bGMYC also gives a more rough subdivision, with 16 major clades only (clades 1–2, 7–8, 9–10, 12–14, 16–17 and 20–21 from the mPTP are not recognized as independent clades in this analysis).

We can roughly estimate the time of differentiation of the *M. micrura* species group (=superclade) as Upper Cretaceous; separation of the 12–14 clade (containing the Arabian

population) took place in the Eocene, and the splitting off of clades 12–13 took place around the Oligocene.

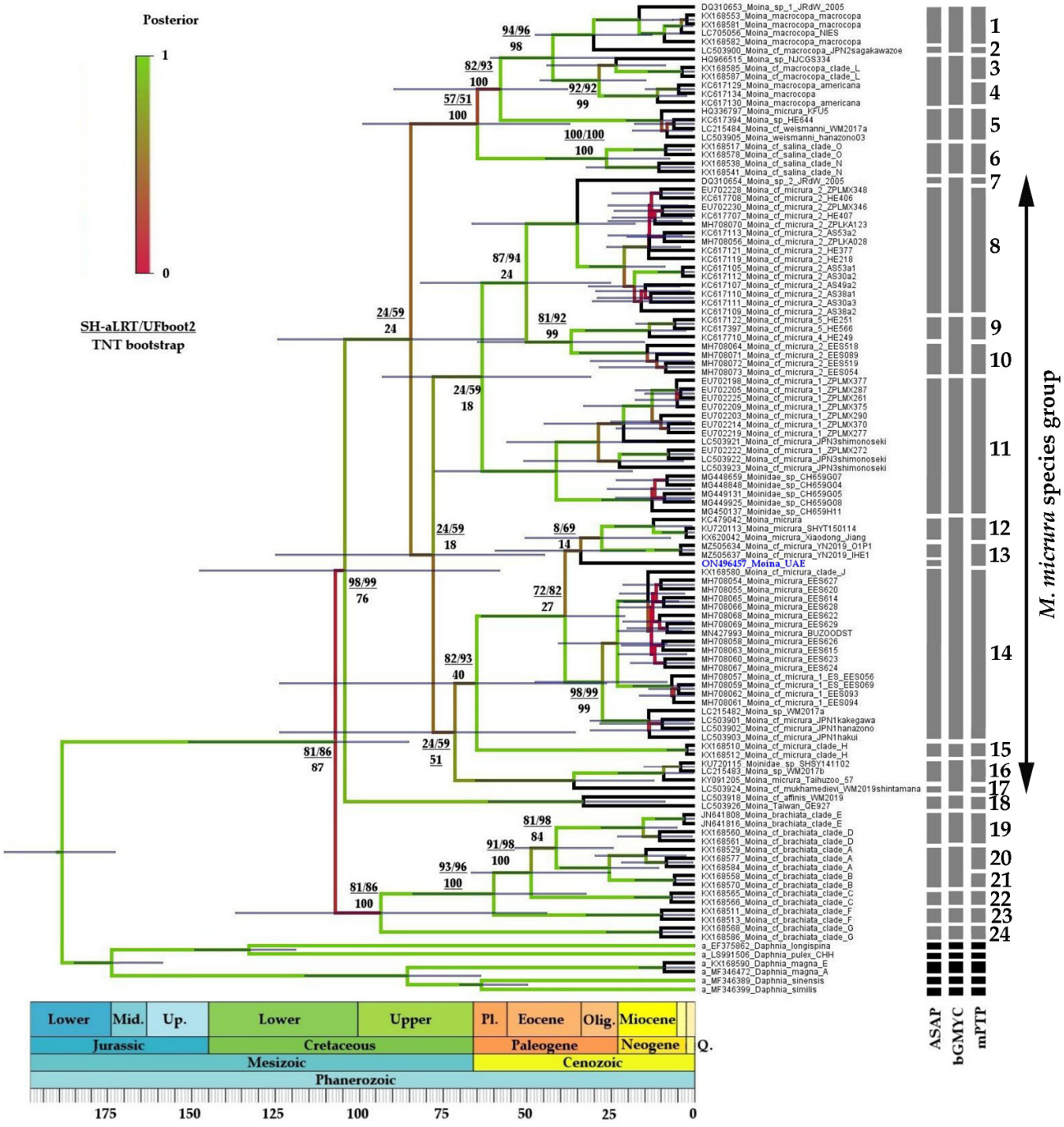

Figure 22. Phylogenetic ultrametric tree based on COI mitochondrial gene for *Moina* with relaxed molecular clock estimates based on fossil calibration points. Sequence from UAE is marked with blue colour. Prior probability of branches is coded by the colour gradient from red (low) to green (high). Node supports for key points are: value of the SH-aLRT for the first digit/value of UFboot2 (ML) for the second digit and standard (TNT) bootstrap value in the denominator. The bars depict the 95% highest probability density (HPD) interval of the estimated divergence times. Results of delimitation based on *p*-distance (ASAP), the Bayesian general coalescence model (bGMYC) and multi-rate Poisson tree processes (mPTP) are represented by grey bars on the right side.

4. Discussion

Not surprisingly, the fauna of the studied water bodies were very poor: only five taxa were found, and the maximum number of taxa per single sample was three. Two previous investigations [40,41], combined with this study plus reports of separate taxa [29,42], revealed *in toto* only five taxa (as *D. carinata* and *A. dentifera* in these publications were apparent misidentifications of *D. arabica* and *C. anemae*) for all studied water bodies, including both field samples and hatched specimens. In contrast to some other regions [82–84], only a few taxa could be hatched from the sediments in Arabian water bodies.

Remarkably, some localities that appeared to be attractive for the development of the cladoceran populations (Figure 1d) were fully lacking them during the sampling time (i.e., late autumn, which seems to be optimal for the sampling of water bodies with significant seasonality due to the more moderate climate compared to the extremely dry summer). In comparison, copepods and ostracods were very numerous there. Soesbergen [41] also found any types of cladocerans only in two artificial concrete ponds, while other water bodies (Wasit Wetland and Wadi Halah) lacked these populations. The explanation that such water bodies were not colonized by the cladocerans due various difficulties in their colonization is unsatisfactory: migrating water fowl (the main vector of the resting egg dispersion [5,10]) have probably visited these areas during the many years of their existence and had a chance to introduce the cladoceran resting eggs. Moreover, it was possible to hatch the additional species that were absent at the sampling time from the dried bottom sediments (i.e., *Anthalona mediterranea* from the mud collected in Masfoot Dam). Most probably, different species of the water fleas in such areas adapted to a very short vegetation season, produced several generations (if not a single generation?), fully switched to the ephippium and male production and then went extinct in the active phase, remaining represented by the ephippia only.

Such a life cycle is possibly a reflection of strong water-body warming during the summer. Very high temperature could be a limiting factor for the development of many cladoceran populations; first of all, those in shallow waters warmed to the bottom during summer. Indeed, the upper temperature limit was determined as about 30 °C for *Daphnia*, *Ceriodaphnia* and *Simocephalus* [85,86]. Moreover, temperatures of about 32–36 °C are 100% lethal for most daphniids [86]. However, there are some exclusions from this rule among other taxa. *Moina macrocopa* survives at 36 °C (but dies at 39–41 °C) [87], and *Latonopsis* normally occurs at 34–38 °C. For some species of *Macrothrix*, the lethal temperature is 50 °C [88,89]. Apparently, the cladocerans found here are among the most thermally resistant on the planet.

To date, *Anthalona mediterranea* is regarded as a taxon locally distributed in desert areas of the Mediterranean region (Turkey), the Arabian Peninsula and Sokotra Island [42]. Similarly, *Coronatella anemae* is found in the desert areas of northeast Africa, the Ababian Peninsula, Sokotra Island and Middle Asia (Uzbekistan) [46,90]. In contrast, two other taxa have a wide distribution in the tropics: *Ceriodaphnia cornuta* group in the tropics and subtropics of different continents, while *Moina micrura* group in the latter zone and even the southern portion of the Boreal zone in different continents [81,90,91]. Among the revealed taxa, only *Daphnia arabica* is very local and micro-endemic (to date, it has been found in a single locality [43]). Such a conclusion was based on few samples, but only a few additional water bodies are available for the ctedodaphniids in this desert region [43].

However, we need to take into consideration the different levels of study of different taxa recorded here. *Daphnia* is a model subject in genetic studies [13,14,92,93], reinforced by morphological revisions [94–96]. Molecular studies are almost absent for the chydorids (with a few exceptions [97–100]), but their morphology-based taxonomy is well-elaborated, including the species groups under consideration [42,46,101–103]. In contrast, morphology-based revisions of the genera *Ceriodaphnia* and *Moina* are rare [80,104,105], and they were almost absent for the *C. cornuta* and *M. micrura* groups, although some wide-range molec-

ular studies have been undertaken [100,106–109]. The width of the distribution ranges is correlated with the unrevised status of the species group.

We do not discuss here the advantages and weaknesses of different delimitation approaches, which we have discussed elsewhere [96,110]. Without taking into account the method of delimitation, most revealed mitochondrial clades in reality represent separate taxa of the *Ceriodaphnia cornuta* complex and of the *Moina micrura* species group. Of course, such conclusions must be confirmed by accurate revisions combining morphological and molecular methods, and this is a special task for the future. To date, morphological differences between presumable species are unknown, but they could be found in the future, as happened for *D. arabica* [43,47] and other species of the *D. sinensis* group [47]. Only pioneer attempts to find such characters have been undertaken to date, and the characters of the ephippium structure have been found to be the most prospective for species discrimination [91,107], while parthenogenetic females seem to be very similar, as is usual among different cladoceran macro taxa [49].

Unfortunately, the sequence datasets for *Coronatella* and *Anthalona* in Genbank and BOLD are too small for adequate phylogenetic studies to accompany clade differentiation dating. However, it is known that the major clades of chydorids are very old [111]. Most probably, the genera *Coronatella* and *Anthalona* are of Late Mesozoic origin, keeping in mind generally accepted ideas about the antiquity of the cladoceran macro taxa [111,112]. We do not know the exact time of differentiation of these genera and their phylogroups inhabiting the Arabian Peninsula. In contrast, our data allow us to make a rough estimation for three planktonic genera: the *C. cornuta* group was differentiated in the Upper Jurassic to Lower Cretaceous, the *M. micrura* group in the Upper Cretaceous and previously we concluded that *D. sinensis* group was differentiated in the Paleocene [43]. Our data suggest that the major clade differentiations within each group took place in the Lower Cretaceous, Eocene and Oligocene–Miocene, respectively. Note that fossil ephippia of *Moina* and *Ceriodaphnia* are known from the Late Mesozoic [49,113], confirming the realism of our estimations.

Note that, similarly to the tree by Ni et al. [109], our tree of *Moina* has low support for deep branches, and we cannot discuss the relationships between the major species groups of this genus here. We can only roughly estimate the time of their differentiation based on our tree because of the calibration points involving another genus (*Daphnia*). The same is true for *Ceriodaphnia*: it was previously shown that the COI tree for this genus also lacks resolution for deep clades [80]. Using our rough estimation, we can conclude that the Arabian clades of *Ceriodaphnia*, *Moina* and *Daphnia* were separated in the Oligocene to Miocene, Oligocene and Early Pleistocene, respectively. Therefore, all clades (of different hierarchical orders) in the Arabian Peninsula are very old compared to the clades of similar rank in Northern Eurasia, which usually have a Late Pleistocene history [114,115].

Unfortunately, we only have very rough ideas about the cladoceran phylogeography in more southern (tropical) territories due to the lack of detailed studies on tropical populations. Currently, the cladoceran fauna of the Arabian Peninsula could be regarded as a collection of phylogenetic relicts [116] of pre-Pleistocene times. At the same time, they possibly represent biogeographic relicts sensu Grandcolas et al. [116], but such a hypothesis needs further checking; i.e., using phylogeographic methods with a wider range of studied populations.

The resolution of this study was low (but it can partly be explained by the rarity of the water bodies in this desert area); however, the revealed pattern has analogies with that previously revealed in the far east of Eurasia, where several local relicts strongly separated genetically from their congeners are found [51,96,117]. Such a pattern appeared as a result of the mass extinction of these groups following the Oligocene (after the "Eocene-Oligocene transition") due to general climate cooling and aridization [118–120]. Surviving freshwater relicts are concentrated in the belt of the subtropics and closest warm areas of the temperate zone [96,121]. The Arabian Peninsula also belongs to this belt, but the genetic separation of the phyloclades surviving after the aforementioned mass extinction was reinforced by stronger aridization following the Miocene caused by the shrinkage of the Tethys Sea and

subsequent changes in the moisture transport sources [122]. This drying was stronger compared to many other subtropical territories, apparently including even hyper-arid periods in the Pleistocene [123], and had a stronger effect on the fauna [124] compared to less arid regions of Eurasia.

Most Arabian species belong to the eurybiotic taxa inhabiting both permanent and temporary water bodies of different types [42,46,47,81]. The same situation is characteristic of the cladocerans from other arid regions of Eurasia; moreover, only *Daphnia* (*Ctenodaphnia*), *Moina* and the *Alona*-like chydorids are dominant there (although *Daphnia* s.str., *Simocephalus*, *Chydorus* and *Macrothrix* are also frequently present in the same localities) [23,80,125,126]. Note that *Macrothrix* was found by Soesbergen [41], although the illustrations represented in this article do not adequately confirm exact species identification—it could be *M.* cf. *hirsuticornis*, also common in the Arid Belt of Eurasia [90].

It was previously shown that the communities only consisting of the aforementioned taxa have persisted unchanged in the Arid Belt of Eurasia for millions of years [127], and analogous communities also existed in Pleistocene Beringia, but then they were replaced by the communities of the modern type [128]. We can hypothesize that the communities of the temporary and semi-permanent waters of the Eurasian Arid Belt (including the Arabian Peninsula) contain relicts of pre-Pleistocene epochs, well-adapted to extremely hot and dry conditions. Most of our sampled water bodies were newly constructed man-made reservoirs. As the revealed phylogroups were locally distributed, we can hypothesize that they are colonists from various surrounding natural water bodies. The latter were inhabited by the relicts of older fauna that survived after the great climate aridization (see [123,129]) and then occupied newly available biotopes. However, new paleolimnological and phylogeographic studies must be conducted in the future to confirm this hypothesis.

The Arabian Peninsula remains poorly studied in relation to the diversity of freshwater microcrustaceans, and the comprehensive inventory of their diversity needs to be continued.

Supplementary Materials: The following supporting information can be downloaded at: https://www.mdpi.com/article/10.3390/d14080688/s1, Table S1: Sequences used in this study.

Author Contributions: Conceptualization, W.H., A.A.K.; methodology, A.N.N., D.P.K.; software, D.P.K.; formal analysis, S.E.S.A.N., A.N.N., W.H.; investigation, W.H., S.E.S.A.N., A.N.N., D.P.K.; resources, S.E.S.A.N.; data curation, S.E.S.A.N., A.A.K.; writing—original draft preparation, W.H., A.N.N., A.A.K.; writing—review and editing, W.H., A.A.K.; visualization, A.N.N., D.P.K.; supervision, W.H.; project administration, W.H., A.N.N.; funding acquisition, A.N.N. All authors have read and agreed to the published version of the manuscript.

Funding: All work in the UAE was self-supported by Waleed Hamza, Biology Department, UAEU; phylogeographic studies were supported by the Russian Science Foundation (grant 22-14-00258).

Institutional Review Board Statement: Not applicable.

Data Availability Statement: The sequences from this study were submitted to the NCBI GenBank database (accession numbers ON437588 and ON496457).

Acknowledgments: All SEM work was carried out at the Joint Usage Center "Instrumental Methods in Ecology" (A.N. Severtsov Institute of Ecology and Evolution of Russian Academy of Sciences). Many thanks to R.J. Shiel for linguistic corrections in an earlier draft.

Conflicts of Interest: The authors declare no conflict of interest. The funders had no role in the design of the study; in the collection, analyses, or interpretation of data; in the writing of the manuscript; or in the decision to publish the results.

References

1. CBD. The Convention on Biological Diversity. Available online: https://www.cbd.int (accessed on 7 July 2022).
2. Norman, M. Biodiversity hotspots hevisited. *Bioscience* **2003**, *53*, 916. [CrossRef]
3. Bellard, C.; Leclerc, C.; Leroy, B.; Bakkenes, M.; Veloz, S.; Thuiller, W.; Courchamp, F. Vulnerability of biodiversity hotspots to global change. *Glob. Ecol. Biogeogr.* **2014**, *23*, 1376–1386. [CrossRef]
4. Maciorowski, G.; Jankowiak, Ł.; Sparks, T.H.; Polakowski, M.; Tryjanowski, P. Biodiversity hotspots at a small scale: The importance of eagles' nests to many other animals. *Ecology* **2021**, *102*, e03220. [CrossRef] [PubMed]
5. Banarescu, P. *Zoogeography of Freshwaters: Volume 1. General Distribution and Dispersal of Freshwater Animals*; AULA-Verlag: Wiesbaden, Germany, 1990; ISBN 3-89104-480-1.
6. Avise, J.C. *Phylogeography: The History and Formation of Species*; Harvard University Press: Cambridge, MA, USA; London, UK, 2000; ISBN 0674666380.
7. McNeely, J.A. Biodiversity in arid regions: Values and perceptions. *J. Arid. Environ.* **2003**, *54*, 61–70. [CrossRef]
8. Tourenq, C.; Launay, F. Challenges facing biodiversity in the United Arab Emirates. *Manag. Environ. Quality* **2008**, *19*, 283–304. [CrossRef]
9. Garcia, N.; Harrison, I.J.; Cox, N.; Tognelli, M.F. (Eds.) *The Status and Distribution of Freshwater Biodiversity in the Arabian Peninsula*; IUCN Solprint: Mijas, Spain, 2015; ISBN 978-2-8317-1706-7.
10. Dumont, H.J.; Negrea, S. Introduction to the class Branchiopoda. In *Guides to the Identification of the Microinvertebrates of the Continental Waters of the World*; Dumont, H.J., Ed.; Backhuys Publications: Leiden, Germany, 2002; ISBN 9057821125.
11. Zawisza, E.; Zawiska, I.; Correa-Metrio, A. Cladocera Community Composition as a Function of Physicochemical and Morphological Parameters of Dystrophic Lakes in NE Poland. *Wetlands* **2016**, *36*, 1131–1142. [CrossRef]
12. Ballinger, M.J.; Bruenn, J.A.; Kotov, A.A.; Taylor, D.J. Selectively maintained paleoviruses in Holarctic water fleas reveal an ancient origin for phleboviruses. *Virology* **2013**, *446*, 276–282. [CrossRef]
13. Ebert, D. Genomics. A genome for the environment. *Science* **2011**, *331*, 539–540. [CrossRef]
14. Ebert, D. Daphnia as a versatile model system in ecology and evolution. *EvoDevo* **2022**, *13*, 16. [CrossRef]
15. Figuerola, J.; Green, A.J. Dispersal of aquatic organisms by waterbirds: A review of past research and priorities for future studies. *Freshw. Biol.* **2002**, *47*, 483–494. [CrossRef]
16. Forro, L.; Korovchinsky, N.M.; Kotov, A.A.; Petrusek, A. Global diversity of cladocerans (Cladocera; Crustacea) in freshwater. *Hydrobiologia* **2008**, *595*, 177–184. [CrossRef]
17. Dumont, H.J.; Maas, S.; Martens, K. Cladocera, Copepoda and Ostracoda (Crustacea) from fresh waters in South Yemen. *Fauna of Saudi Arabia* **1986**, *8*, 12–19.
18. Dumont, H.J.; Brancelj, A. Alona alsafadii n. sp. from Yemen, a primitive, groundwater-dwelling member of the A. karua-group. *Hydrobiologia* **1994**, *281*, 57–64. [CrossRef]
19. Schmarda, L.K. Zur Naturgeschichte Agyptens. *Denksch. K. Akad. Wiss. Math. Nat. Cl.* **1854**, *VII*, 1–28.
20. Blanchard, R.; Richard, J. Sur les crustaces des Sebkhaset des chotts d'Algerie. *Bull. Soc. Zool. Fr.* **1890**, *15*, 136–138.
21. Ekman, S. Cladoceren und freilebende Copepoden aus Agypten und dem Sudan. In *Results of the Swedish Zoological Expedition to Egypt and the White Nile, 1901, under the Direction of L.A. Jagerskiold*; Jagerskiold, L.A., Ed.; Library of the Royal University of Uppsala: Uppsala, Sweden, 1904; pp. 1–18.
22. Gurney, R. X—On the fresh-water Crustacea of Algeria and Tunisia. *J. R. Micr. Soc.* **1909**, *29*, 273–305. [CrossRef]
23. Gauthier, H. Ostracodes et Cladocères de l'Afrique du Nord, deuxieme note. *Bull. Soc. Hist. Nat. Afr. Nord.* **1928**, *19*, 69–79.
24. Harding, J.P. The Armstrong College zoological expedition to Siwa Oasis (Libyan Desert) 1935. Crustacea: Branchiopoda and Ostracoda. *Proc. Egypt. Acad. Sci.* **1955**, *10*, 58–68.
25. Dumont, H.J.; Laureys, P.; Pensaert, J. Anostraca, Conchostraca, Cladocera and Copepoda from Tunisia. *Hydrobiologia* **1979**, *66*, 259–274. [CrossRef]
26. Samraoui, B.; Segers, H.; Maas, S.; Baribwegure, D.; Dumont, H.J. Rotifera, Cladocera, Copepoda, and Ostracoda from coastal wetlands in northeast Algeria. *Hydrobiologia* **1998**, *386*, 183–193. [CrossRef]
27. Marrone, F.; Korn, M.; Stoch, F.; Naselli-Flores, L.; Turki, S. Updated checklist and distribution of large branchiopods (Branchiopoda: Anostraca, Notostraca, Spinicaudata) in Tunisia. *Biogeographia* **2016**, 27–53. [CrossRef]
28. Ghaouaci, S.; Amarouayache, M.; Sinev, A.Y.; Korovchinsky, N.M.; Kotov, A.A. An annotated checklist of the Algerian Cladocera (Crustacea: Branchiopoda). *Zootaxa* **2018**, *4377*, 412–430. [CrossRef]
29. Van Damme, K.; Dumont, H.J. A new species of Moina Baird, 1950 (Crustacea: Anomopoda) from Socotra Island, Yemen. *Zootaxa* **2008**, *1721*, 24. [CrossRef]
30. Madera, P.; Van Damme, K. Socotra Archipelago (Yemen). In *Imperiled: The Encyclopedia of Conservation*; DellaSala, D.A., Goldstein, M.I., Eds.; Elsevier: Amsterdam, The Netherlands, 2022; pp. 267–281. ISBN 9780128211397.
31. Abell, R.; Thieme, M.L.; Revenga, C.; Bryer, M.; Kottelat, M.; Bogutskaya, N.; Coad, B.; Mandrak, N.; Balderas, S.C.; Bussing, W.; et al. Freshwater ecoregions of the World: A new map of biogeographic units for freshwater biodiversity Conservation. *Bioscience* **2008**, *58*, 403–414. [CrossRef]
32. FEOW. Freshwater Ecoregions of the World. Available online: https://www.feow.org/ (accessed on 7 July 2022).
33. Dinerstein, E.; Olson, D.; Joshi, A.; Vynne, C.; Burgess, N.D.; Wikramanayake, E.; Hahn, N.; Palminteri, S.; Hedao, P.; Noss, R.; et al. An ecoregion-based approach to protecting half the terrestrial realm. *Bioscience* **2017**, *67*, 534–545. [CrossRef]

34. Feulner, G.R. Wadi fish of the UAE. *Tribulus* **1998**, *8*, 16–22.
35. Feulner, G.R.; Green, S.A. Freshwater snails of the UAE. *Tribulus* **1999**, *9*, 5–9.
36. Saji, A.; Mischke, S.; Soorae, P.S.; Ahmed, S.; Al Dhaheri, S. The alwathba wetland reserve lake in Abu Dhabi, United Arab Emirates and its ostracod (seed shrimp) fauna. *Int. J. Aquat. Biol.* **2018**, *6*, 265–273. [CrossRef]
37. Saji, A.; Al Dhaheri, S.; Shah, J.N.; Soorae, P.S. Influence of chemical parameters on Artemia sp. (Crustacea: Anostraca) population in Al Wathba Lake in the Abu Dhabi Emirate, UAE. *Int. J. Aquat. Biol.* **2016**, *4*, 87–95. [CrossRef]
38. Asem, A.; Schuster, R.; Eimanifar, A.; Lu, H.; Liu, C.; Wu, X.; Yao, L.; Meng, X.; Li, W.; Wang, P. Impact of colonization of an invasive species on genetic differentiation in new environments: A study on American Artemia franciscana (Crustacea: Anostraca) in the United Arab Emirates. *J. Ocean Univ. China* **2021**, *20*, 911–920. [CrossRef]
39. Soorae, P.; Javed, S.; Dhaheri, S.A.; Qassimi, M.A.; Kabshawi, M.; Saji, A.; Khan, S.; Sakkir, S.; Zaabi, R.A.; Ahmed, S.; et al. Alien species recorded in the United Arab Emirates: An initial list of terrestrial and freshwater species. *J. Threat. Taxa* **2015**, *7*, 7910–7921. [CrossRef]
40. Hamza, W.; Ramadan, G.; AlKaabi, M. Morphological and molecular identification of first recorded Cladoceran organisms in the desert of Abu Dhabi, UAE. *MOJ Eco. Environ. Sci.* **2018**, *3*, 220–224. [CrossRef]
41. Soesbergen, M. A preliminary investigation of plankton organisms of fresh and brackish inland waters in the northern United Arab Emirates. *Tribulus* **2018**, *26*, 46–58.
42. Van Damme, K.; Sinev, A.Y.; Dumont, H.J. Separation of Anthalona gen.n. from Alona Baird, 1843 (Branchiopoda: Cladocera: Anomopoda): Morphology and evolution of scraping stenothermic alonines. *Zootaxa* **2011**, *2875*, 1–64. [CrossRef]
43. Hamza, W.; Neretina, A.N.; Al Neyadi, S.E.S.; Amiri, K.; Karabanov, D.P.; Kotov, A.A. Discovery of a New Species of Daphnia (Crustacea: Cladocera) from the Arabian Peninsula Revealed a Southern Origin of a Common Northern Eurasian Species Group. *Water* **2022**, *14*, 2350. [CrossRef]
44. Sayers, E.W.; Cavanaugh, M.; Clark, K.; Ostell, J.; Pruitt, K.D.; Karsch-Mizrachi, I. GenBank. *Nucleic Acids Res.* **2019**, *47*, D94–D99. [CrossRef]
45. Ratnasingham, S.; Hebert, P.D.N. BOLD: The Barcode of Life Data System. *Mol. Ecol. Notes* **2007**, *7*, 355–364. [CrossRef]
46. Van Damme, K.; Dumont, H.J. Further division of Alona Baird, 1843: Separation and position of Coronatella Dybowski et Grochowski and Ovalona gen.n. (Crustacea: Cladocera). *Zootaxa* **2008**, *1960*, 1–44. [CrossRef]
47. Popova, E.V.; Petrusek, A.; Korinek, V.; Mergeay, J.; Bekker, E.I.; Karabanov, D.P.; Galimov, Y.R.; Neretina, T.V.; Taylor, D.J.; Kotov, A.A. Revision of the Old World Daphnia (Ctenodaphnia) similis group (Cladocera: Daphniidae). *Zootaxa* **2016**, *4161*, 1–40. [CrossRef]
48. Korovchinsky, N.M.; Kotov, A.A.; Sinev, A.Y.; Neretina, A.N.; Garibian, P.G. *Water Fleas (Crustacea: Cladocera) of Northern Eurasi*; KMK Scientific Press Ltd.: Moscow, Russia, 2021; Volume 2, ISBN 978-5-907372-50-4.
49. Kotov, A.A. *Morphology and Phylogeny of the Anomopoda (Crustacea: Cladocera)*; KMK Scientific Press Ltd.: Moscow, Russia, 2013; ISBN 9785873179237.
50. Hebert, P.D.N.; Cywinska, A.; Ball, S.L.; deWaard, J.R. Biological identifications through DNA barcodes. *Proc. R. Soc. Lond. B Biol. Sci.* **2003**, *270*, 313–321. [CrossRef]
51. Neretina, A.N.; Karabanov, D.P.; Sacherova, V.; Kotov, A.A. Unexpected mitochondrial lineage diversity within the genus Alonella Sars, 1862 (Crustacea: Cladocera) across the Northern Hemisphere. *PeerJ* **2021**, *9*, e10804. [CrossRef]
52. Okonechnikov, K.; Golosova, O.; Fursov, M. Unipro UGENE: A unified bioinformatics toolkit. *Bioinformatics* **2012**, *28*, 1166–1167. [CrossRef]
53. Sayers, E.W.; Beck, J.; Brister, J.R.; Bolton, E.E.; Canese, K.; Comeau, D.C.; Funk, K.; Ketter, A.; Kim, S.; Kimchi, A.; et al. Database resources of the National Center for Biotechnology Information. *Nucleic Acids Res.* **2020**, *48*, D9–D16. [CrossRef]
54. Katoh, K.; Standley, D.M. MAFFT multiple sequence alignment software version 7: Improvements in performance and usability. *Mol. Biol. Evol.* **2013**, *30*, 772–780. [CrossRef]
55. Kalyaanamoorthy, S.; Minh, B.Q.; Wong, T.K.F.; von Haeseler, A.; Jermiin, L.S. ModelFinder: Fast model selection for accurate phylogenetic estimates. *Nat. Methods* **2017**, *14*, 587–589. [CrossRef]
56. Trifinopoulos, J.; Nguyen, L.-T.; von Haeseler, A.; Minh, B.Q. W-IQ-TREE: A fast online phylogenetic tool for maximum likelihood analysis. *Nucleic Acids Res.* **2016**, *44*, W232–W235. [CrossRef]
57. Posada, D.; Buckley, T.R. Model selection and model averaging in phylogenetics: Advantages of Akaike information criterion and Bayesian approaches over likelihood ratio tests. *Syst. Biol.* **2004**, *53*, 793–808. [CrossRef] [PubMed]
58. Yang, Z.; Rannala, B. Molecular phylogenetics: Principles and practice. *Nat. Rev. Genet.* **2012**, *13*, 303–314. [CrossRef] [PubMed]
59. Vaidya, G.; Lohman, D.J.; Meier, R. SequenceMatrix: Concatenation software for the fast assembly of multi-gene datasets with character set and codon information. *Cladistics* **2011**, *27*, 171–180. [CrossRef] [PubMed]
60. Minh, B.Q.; Schmidt, H.A.; Chernomor, O.; Schrempf, D.; Woodhams, M.D.; von Haeseler, A.; Lanfear, R. IQ-TREE 2: New models and efficient methods for phylogenetic inference in the genomic era. *Mol. Biol. Evol.* **2020**, *37*, 1530–1534. [CrossRef]
61. Hoang, D.T.; Chernomor, O.; von Haeseler, A.; Minh, B.Q.; Le Vinh, S. UFBoot2: Improving the ultrafast bootstrap approximation. *Mol. Biol. Evol.* **2018**, *35*, 518–522. [CrossRef]
62. Guindon, S.; Dufayard, J.-F.; Lefort, V.; Anisimova, M.; Hordijk, W.; Gascuel, O. New algorithms and methods to estimate maximum-likelihood phylogenies: Assessing the performance of PhyML 3.0. *Syst. Biol.* **2010**, *59*, 307–321. [CrossRef]

63. Goloboff, P.A.; Catalano, S.A. TNT version 1.5, including a full implementation of phylogenetic morphometrics. *Cladistics* **2016**, *32*, 221–238. [CrossRef]
64. Heled, J.; Drummond, A.J. Bayesian inference of species trees from multilocus data. *Mol. Biol. Evol.* **2010**, *27*, 570–580. [CrossRef]
65. Bouckaert, R.; Vaughan, T.G.; Barido-Sottani, J.; Duchene, S.; Fourment, M.; Gavryushkina, A.; Heled, J.; Jones, G.; Kuhnert, D.; de Maio, N.; et al. BEAST 2.5: An advanced software platform for Bayesian evolutionary analysis. *PLoS Comput. Biol.* **2019**, *15*, e1006650. [CrossRef]
66. Drummond, A.J.; Suchard, M.A.; Xie, D.; Rambaut, A. Bayesian phylogenetics with BEAUti and the BEAST 1.7. *Mol. Biol. Evol.* **2012**, *29*, 1969–1973. [CrossRef]
67. Cornetti, L.; Fields, P.D.; Van Damme, K.; Ebert, D. A fossil-calibrated phylogenomic analysis of Daphnia and the Daphniidae. *Mol. Phylogenet. Evol.* **2019**, *137*, 250–262. [CrossRef]
68. Rambaut, A.; Drummond, A.J.; Xie, D.; Baele, G.; Suchard, M.A. Posterior summarization in Bayesian phylogenetics using Tracer 1.7. *Syst. Biol.* **2018**, *67*, 901–904. [CrossRef]
69. Drummond, A.J.; Bouckaert, R.R. *Bayesian Evolutionary Analysis with BEAST2*; Cambridge University Press: Cambridge, UK, 2015; ISBN 978-1-107-01965-2.
70. Parham, J.F.; Donoghue, P.C.J.; Bell, C.J.; Calway, T.D.; Head, J.J.; Holroyd, P.A.; Inoue, J.G.; Irmis, R.B.; Joyce, W.G.; Ksepka, D.T.; et al. Best practices for justifying fossil calibrations. *Syst. Biol.* **2012**, *61*, 346–359. [CrossRef]
71. Douglas, J.; Zhang, R.; Bouckaert, R. Adaptive dating and fast proposals: Revisiting the phylogenetic relaxed clock model. *PLoS Comput. Biol.* **2021**, *17*, e1008322. [CrossRef]
72. Gernhard, T. The conditioned reconstructed process. *J. Theor. Biol.* **2008**, *253*, 769–778. [CrossRef]
73. Barido-Sottani, J.; Boskova, V.; Du Plessis, L.; Kuhnert, D.; Magnus, C.; Mitov, V.; Muller, N.F.; PecErska, J.; Rasmussen, D.A.; Zhang, C.; et al. Taming the BEAST—A community teaching material resource for BEAST2. *Syst. Biol.* **2018**, *67*, 170–174. [CrossRef] [PubMed]
74. Puillandre, N.; Brouillet, S.; Achaz, G. ASAP: Assemble species by automatic partitioning. *Mol. Ecol. Resour.* **2021**, *21*, 609–620. [CrossRef] [PubMed]
75. Pons, J.; Barraclough, T.G.; Gomez-Zurita, J.; Cardoso, A.; Duran, D.P.; Hazell, S.; Kamoun, S.; Sumlin, W.D.; Vogler, A.P. Sequence-based species delimitation for the DNA taxonomy of undescribed insects. *Syst. Biol.* **2006**, *55*, 595–609. [CrossRef] [PubMed]
76. Reid, N.M.; Carstens, B.C. Phylogenetic estimation error can decrease the accuracy of species delimitation: A Bayesian implementation of the general mixed Yule-coalescent model. *BMC Evol. Biol.* **2012**, *12*, 196. [CrossRef]
77. *Microsoft R Open Application Network*; Microsoft, R. Core Team: Redmond, DC, USA, 2014.
78. Carstens, B.C.; Pelletier, T.A.; Reid, N.M.; Satler, J.D. How to fail at species delimitation. *Mol. Ecol.* **2013**, *22*, 4369–4383. [CrossRef]
79. Kapli, P.; Lutteropp, S.; Zhang, J.; Kobert, K.; Pavlidis, P.; Stamatakis, A.; Flouri, T. Multi-rate Poisson tree processes for single-locus species delimitation under maximum likelihood and Markov chain Monte Carlo. *Bioinformatics* **2017**, *33*, 1630–1638. [CrossRef]
80. Alonso, M.; Neretina, A.N.; Ventura, M. Ceriodaphnia smirnovi (Crustacea: Cladocera), a new species from the Mediterranean region, and a phylogenetic analysis of the commonest species. *Zootaxa* **2021**, *4974*, 146. [CrossRef]
81. Smirnov, N.N. *Macrothricidae i Moinidae fauni mira. Fauna SSSR. Rakoobraznye. [Macrothricidae and Moinidae of the World's fauna. Fauna of the USSR. Crustacea]*; Nauka: Leningrad, Russia, 1976.
82. Sars, G.O. Contributions to the knowledge of the fresh-water Entomostraca of South America, as shown by artificial hatching from dried material. *Arch. Math. Naturvid. B* **1901**, *XXIII*, 1–102.
83. Van Damme, K.; Dumont, H.J. Cladocera of the Lencois Maranhenses (NE—Brazil): Faunal composition and a reappraisal of Sars' Method. *Braz. J. Biol.* **2010**, *70*, 755–779. [CrossRef]
84. Diniz, L.P.; Melo-Junior, M.D. Can nearby eutrophic reservoirs sustain a differentiated biodiversity of planktonic microcrustaceans in a tropical semiarid basin? *An. Acad. Bras. Cienc.* **2017**, *89*, 2771–2783. [CrossRef]
85. Mallin, M.A.; Partin, W.E. Thermal tolerances of common Cladocera. *J. Freshw. Ecol.* **1989**, *5*, 45–51. [CrossRef]
86. Smirnov, N.N. *Physiology of the Cladocera*, 2nd ed.; Academic Press: Amsterdam, The Netherlands, 2017; ISBN 9780128051948.
87. Maksimova, L.P. *Instructions on cultivation of Moina macrocopa Straus*; GosNIORKh: Leningrad, Russia, 1969.
88. Korovchinsky, N.M. *Cladocerans of the Order Ctenopoda of the World Fauna (Morphology, Systematics, Ecology, Biogeography)*; KMK Press: Moscow, Russia, 2004.
89. Brown, L.A. The natural history of Cladocerans in relation to temperature. I. Distribution and the temperature limits for vital activities. *Am. Nat.* **1929**, *63*, 248–264. [CrossRef]
90. Korovchinsky, N.M.; Kotov, A.A.; Boikova, O.S.; Smirnov, N.N. *Water Fleas (Crustacea: Cladocera) of Northern Eurasia*; KMK Scientific Press Ltd.: Moscow, Russia, 2021; Volume 1, ISBN 978-5-907372-27-6.
91. Berner, D.B. Morphological differentiation among species in the Ceriodaphnia cornuta complex (Crustacea, Cladocera). *Verh. Internat. Verein. Limnol.* **1985**, *22*, 3099–3103. [CrossRef]
92. Adamowicz, S.J.; Petrusek, A.; Colbourne, J.K.; Hebert, P.D.N.; Witt, J.D.S. The scale of divergence: A phylogenetic appraisal of intercontinental allopatric speciation in a passively dispersed freshwater zooplankton genus. *Mol. Phylogenet. Evol.* **2009**, *50*, 423–436. [CrossRef] [PubMed]

93. Bekker, E.I.; Karabanov, D.P.; Galimov, Y.R.; Haag, C.R.; Neretina, T.V.; Kotov, A.A. Phylogeography of Daphnia magna Straus (Crustacea: Cladocera) in Northern Eurasia: Evidence for a deep longitudinal split between mitochondrial lineages. *PLoS ONE* **2018**, *13*, e0194045. [CrossRef]
94. Juracka, P.J.; Laforsch, C.; Petrusek, A. Neckteeth formation in two species of the Daphnia curvirostris complex (Crustacea: Cladocera). *J. Limnol.* **2011**, *70*, 359–368. [CrossRef]
95. Zuykova, E.I.; Simonov, E.P.; Bochkarev, N.A.; Taylor, D.J.; Kotov, A.A. Resolution of the Daphnia umbra problem (Crustacea: Cladocera) using an integrated taxonomic approach. *Zool. J. Linn. Soc.* **2018**, *50*, 969–998. [CrossRef]
96. Kotov, A.A.; Garibian, P.G.; Bekker, E.I.; Taylor, D.J.; Karabanov, D.P. A new species group from the Daphnia curvirostris species complex (Cladocera: Anomopoda) from the eastern Palaearctic: Taxonomy, phylogeny and phylogeography. *Zool. J. Linn. Soc.* **2021**, *191*, 772–822. [CrossRef]
97. Gu, Y.-L.; Sun, C.-H.; Liu, P.; Zhang, X.; Sinev, A.Y.; Dumont, H.J.; Han, B.-P. Complete mitochondrial genome of Ovalona pulchella (Branchiopoda, Cladocera) as the first representative in the family Chydoridae: Gene rearrangements and phylogenetic analysis of Cladocera. *Gene* **2022**, *818*, 146230. [CrossRef]
98. Sinev, A.Y.; Karabanov, D.P.; Kotov, A.A. A new North Eurasian species of the Alona affinis complex (Cladocera: Chydoridae). *Zootaxa* **2020**, *4767*, 115–137. [CrossRef]
99. Elias-Gutierrez, M.; Valdez–Moreno, M. A new cryptic species of Leberis Smirnov, 1989 (Crustacea, Cladocera, Chydoridae) from the Mexican semi-desert region, highlighted by DNA barcoding. *Hidrobiologica* **2008**, *18*, 63–74.
100. Bekker, E.I.; Karabanov, D.P.; Galimov, Y.R.; Kotov, A.A. DNA barcoding reveals high cryptic diversity in the North Eurasian Moina species (Crustacea: Cladocera). *PLoS ONE* **2016**, *11*, e0161737. [CrossRef]
101. Sousa, F.D.R.; Elmoor-Loureiro, L.M.A.; Santos, S. Redescription of Coronatella poppei (Richard, 1897) (Crustacea, Branchiopoda, Chydoridae) and a revision of the genus in Brazil, with descriptions of new taxa. *Zootaxa* **2015**, *3955*, 211–244. [CrossRef]
102. Sousa, F.D.R.; Elmoor-Loureiro, L.M.A.; Santos, S. Position of the dentifera-group in the Coronatella-branch and its relocation to a new genus: Magnospina gen. n. (Crustacea, Chydoridae, Aloninae). *Zookeys* **2016**, *586*, 95–119. [CrossRef]
103. Sinev, A.Y. Revision of the elegans-group of Alona s. lato and its status as a subgenus of Coronatella Dybowski et Grochowski, 1894 (Cladocera: Anomopoda: Chydoridae). *Zootaxa* **2020**, *4732*, 501–526. [CrossRef]
104. Neretina, A.N.; Kirdyasheva, A.G. A redescription of Moina australiensis Sars, 1896 (Cladocera: Moinidae) with short notes on Australian moinids. *Zootaxa* **2019**, *4577*, zootaxa.4577.1.10. [CrossRef]
105. Alonso, M.; Neretina, A.N.; Sanoamuang, L.-O.; Saengphan, N.; Kotov, A.A. A new species of Moina Baird, 1850 (Cladocera: Moinidae) from Thailand. *Zootaxa* **2019**, *4554*, 199–218. [CrossRef]
106. Sharma, P.; Kotov, A.A. Molecular approach to identify sibling species of the Ceriodaphnia cornuta complex (Cladocera: Daphniidae) from Australia with notes on the continental endemism of this group. *Zootaxa* **2013**, *3702*, 79–89. [CrossRef]
107. Elias-Gutierrez, M.; Juracka, P.J.; Montoliu-Elena, L.; Miracle, M.R.; Petrusek, A.; Korinek, V. Who is Moina micrura? Redescription of one of the most confusing cladocerans from terra typica, based on integrative taxonomy. *Limnetica* **2019**, *38*, 227–252. [CrossRef]
108. Montoliu-Elena, L.; Elias-Gutierrez, M.; Silva-Briano, M. Moina macrocopa (Straus, 1820): A species complex of a common Cladocera, highlighted by morphology and DNA barcodes. *Limnetica* **2019**, *1*, 253–277. [CrossRef]
109. Ni, Y.; Ma, X.; Hu, W.; Blair, D.; Yin, M. New lineages and old species: Lineage diversity and regional distribution of Moina (Crustacea: Cladocera) in China. *Mol. Phylogenet. Evol.* **2019**, *134*, 87–98. [CrossRef] [PubMed]
110. Luo, A.; Ling, C.; Ho, S.Y.W.; Zhu, C.-D. Comparison of methods for molecular species delimitation across a range of speciation scenarios. *Syst. Biol.* **2018**, *67*, 830–846. [CrossRef] [PubMed]
111. Sacherova, V.; Hebert, P.D.N. The evolutionary history of the Chydoridae (Crustacea: Cladocera). *Biol. J. Linn. Soc.* **2003**, *79*, 629–643. [CrossRef]
112. Van Damme, K.; Kotov, A.A. The fossil record of the Cladocera (Crustacea: Branchiopoda): Evidence and hypotheses. *Earth. Sci. Rev.* **2016**, *163*, 162–189. [CrossRef]
113. Hegna, T.A.; Kotov, A.A. Ephippia belonging to Ceriodaphnia Dana, 1853 (Cladocera: Anomopoda: Daphniidae) from the Lower Cretaceous of Australia. *Palaeontol. Electron.* **2016**, *19*, 1–9. [CrossRef]
114. Kotov, A.A.; Karabanov, D.P.; Bekker, E.I.; Neretina, T.V.; Taylor, D.J. Phylogeography of the Chydorus sphaericus Group (Cladocera: Chydoridae) in the Northern Palearctic. *PLoS ONE* **2016**, *11*, e0168711. [CrossRef]
115. Zuykova, E.I.; Simonov, E.P.; Bochkarev, N.A.; Abramov, S.A.; Sheveleva, N.G.; Kotov, A.A. Contrasting phylogeographic patterns and demographic history in closely related species of Daphnia longispina group (Crustacea: Cladocera) with focus on North-Eastern Eurasia. *PLoS ONE* **2018**, *13*, e0207347. [CrossRef]
116. Grandcolas, P.; Nattier, R.; Trewick, S. Relict species: A relict concept? *Trends Ecol. Evol.* **2014**, *29*, 655–663. [CrossRef]
117. Garibian, P.G.; Karabanov, D.P.; Neretina, A.N.; Taylor, D.J.; Kotov, A.A. Bosminopsis deitersi (Crustacea: Cladocera) as an ancient species group: A revision. *PeerJ* **2021**, *9*, e11310. [CrossRef]
118. Zanazzi, A.; Kohn, M.J.; MacFadden, B.J.; Terry, D.O. Large temperature drop across the Eocene-Oligocene transition in central North America. *Nature* **2007**, *445*, 639–642. [CrossRef]
119. Pekar, S.F.; Christie-Blick, N. Resolving apparent conflicts between oceanographic and Antarctic climate records and evidence for a decrease in pCO_2 during the Oligocene through early Miocene (34–16 Ma). *Palaeogeogr. Palaeoclimatol. Palaeoecol.* **2008**, *260*, 41–49. [CrossRef]

120. Li, S.; Xing, Y.; Valdes, P.J.; Huang, Y.; Su, T.; Farnsworth, A.; Lunt, D.J.; Tang, H.; Kennedy, A.T.; Zhou, Z. Oligocene climate signals and forcings in Eurasia revealed by plant macrofossil and modelling results. *Gondwana Res.* **2018**, *61*, 115–127. [CrossRef]
121. Korovchinsky, N.M. The Cladocera (Crustacea: Branchiopoda) as a relict group. *Zool. J. Linn. Soc.* **2006**, *147*, 109–124. [CrossRef]
122. Zhang, Z.; Ramstein, G.; Schuster, M.; Li, C.; Contoux, C.; Yan, Q. Aridification of the Sahara desert caused by Tethys Sea shrinkage during the Late Miocene. *Nature* **2014**, *513*, 401–404. [CrossRef]
123. Hoelzmann, P.; Gasse, F.; Dupont, L.M.; Salzmann, U.; Staubwasser, M.; Leuschner, D.C.; Sirocko, F. Palaeoenvironmental changes in the arid and sub arid belt (Sahara-Sahel-Arabian Peninsula) from 150 kyr to present. In *Past Climate Variability through Europe and Africa*; Smol, J.P., Last, W.M., Battarbee, R.W., Gasse, F., Stickley, C.E., Eds.; Springer Netherlands & Dordrecht: Dordrecht, The Netherlands, 2004; pp. 219–256. ISBN 978-1-4020-2120-6.
124. Groucutt, H.S.; Petraglia, M.D. The prehistory of the Arabian peninsula: Deserts, dispersals, and demography. *Evol. Anthropol.* **2012**, *21*, 113–125. [CrossRef]
125. Keiser, N. Uber die Cladoceren und Copepoden der Wuste Kara-Kum. *Int. Revue ges. Hydrobiol. Hydrogr.* **1931**, *25*, 355–372. [CrossRef]
126. Gauthier, H. Euphyllopodes et Cladoceres continentaux recoltes par M. Monod au Sahara occidental et en Mauritanie. *Bull. Soc. Sci. Nat. Phys. Maroc* **1937**, *17*, 75–98.
127. Zharov, A.A.; Neretina, A.N.; Rogers, D.C.; Reshetova, S.A.; Sinitsa, S.M.; Kotov, A.A. Pleistocene Branchiopods (Cladocera, Anostraca) from Transbaikalian Siberia demonstrate morphological and ecological stasis. *Water* **2020**, *12*, 3063. [CrossRef]
128. Neretina, A.N.; Gololobova, M.A.; Neplyukhina, A.A.; Zharov, A.A.; Rogers, C.D.; Horne, D.J.; Protopopov, A.V.; Kotov, A.A. Crustacean remains from the Yuka mammoth raise questions about non-analogue freshwater communities in the Beringian region during the Pleistocene. *Sci. Rep.* **2020**, *10*, 859. [CrossRef]
129. Dumont, H.J. Relict distribution patterns of aquatic animals: Another tool in evaluating Late Pleistocene climate changes in the Sahara and Sahel. In *Palaeoecology of Africa and the Surrounding Islands*, 1st ed.; Routledge: Milton Park, UK, 1982; Volume 14, ISBN 9780203744529.